International Journal of Earth Sciences Knowledge and Applications
journal homepage: http://www.ijeska.com/index.php/ijeska

Research Article

e-ISSN: 2687-5993

Novel Ellipsoidal Heights Predictive Models Based on Artificial Intelligence Training Algorithms and Classical Regression Models Techniques: A Case Study in the Greater Kumasi Metropolitan Area Local Geodetic Reference Network, Kumasi, Ghana

Daniel Asenso-Gyambibi[1], Naa Lamkai[1], Michael Stanley Peprah[2], Edwin Kojo Larbi[1], Benedict Asamoah[1], Philip Okantey[1]

[1]*Geo-Informatics Division, Building and Road Research Institute (CSIR-BRRI), Kumasi, Ghana*
[2]*Department of Geomatic Engineering, University of Mines and Technology, Tarkwa, Ghana*

INFORMATION

Article history
Received 08 November 2022
Revised 26 December 2022
Accepted 26 December 2022

Keywords
Artificial Intelligence
Geodetic Reference Network
Height systems
Performance Criteria Indices
Statistical Hypothesis
Regression Models

Contact
*Daniel Asenso-Gyambibi
director@csir.brri.org

ABSTRACT

The standard forward transformation for the direct conversion of curvilinear geodetic coordinates (φ, γ, H) to its associated Cartesian coordinates (E, N, Z) has become a major challenge in most countries. This is due to the non-existence of the ellipsoidal height (h) in the modelling of their local geodetic reference network. Numerous studies in the past and recent years have suggested various mathematical techniques for predicting and estimating local ellipsoidal heights. Primary data used for the studies comprises of topographic data obtained from a survey in the Ghana urban water supply project in the Greater Kumasi Metropolitan Area (GKMA).This study considered an empirical evaluation of soft computing techniques such as Back Propagation Artificial Neural Network (BPANN), Generalized Regression Neural Network (GRNN), Radial Basis Function Artificial Neural Network (RBFANN) and conventional methods such as Polynomial Regression Model (PRM), Autoregressive Integrated Moving Average (ARIMA) and Least Square Regression (LSR). The motive is to apply and assess for the first time in our study area, the working efficiency of the aforementioned techniques. Each model technique was assessed based on statistical hypothesis (F, t) tests and performance criteria indices such as arithmetic mean error (AME), arithmetic mean square error (AMSE), minimum and maximum error value, and arithmetic standard deviation (ASD). The statistical analysis of the results revealed that, RBFANN, GRNN, BPANN, LSR, ARIMA and PRM, successfully estimated the ellipsoidal heights for the study area. However, the ANN models (RBFANN, BPANN, GRNN) outperforms the conventional models (LSR, PRM, ARIMA) in terms of accuracy and precision in estimating the local ellipsoidal heights. Also, statistical findings revealed that RBFANN produced more reliable results compared with the other methods. The main conclusion drawn from this study is that, the method of using soft computing is very much promising and can be adopted to solve some of the major problems related to height issues in Ghana. This study seeks to contribute to the existing knowledge on establishing a precise geodetic vertical datum in Ghana for national heightening purpose.

1. Introduction

Satellites orbiting about the center of gravity of the earth can only measure heights relative to a geocentric reference ellipsoid (Fusami et al., 2021). The h determination for national heightening has been one of the major ongoing research focuses among geodesist, geophysicist, surveyors, topographers and numerous researchers. The essence is that, these heights are important for practical applications in geodesy, surveying, photogrammetry, Geographic Information Systems (GIS), and engineering surveys in the areas of 3-Dimensional (3D) modelling, topographical mapping, structural health monitoring, road and building

construction, extraction of metallic minerals, modeling of geometric geoid (Gucek and Basic, 2009; Konakoglu and Cakir, 2018; Kumi-Boateng and Peprah, 2020; Yilmaz et al., 2017). Ellipsoidal height system provides a compatible vertical model with a global height system for studies in geodynamics and geo-hazard processes (Bihter, 2011). Also, these heights are important due to their geocentric and physical significance (Herbert and Ono, 2018) and very useful for geometric correction of high-resolution satellite images and Synthetic Aperture Radar (SAR) (Falchi et al., 2018).

Ghana's local geodetic reference network is based on the War Office 1926 ellipsoid with data in latitude, longitude and orthometric height (φ, γ, H) without the existence of ellipsoidal height (h) (Ziggah et al., 2016). This is because most local geodetic networks were established at a time where satellite positioning techniques have not reached the advanced stage (Ziggah et al., 2016). Hence, measured distances, angles and local datum points of most countries were fixed on the basis of astronomical observations, traversing and terrestrial triangulation (Constantin-Octavian, 2006).

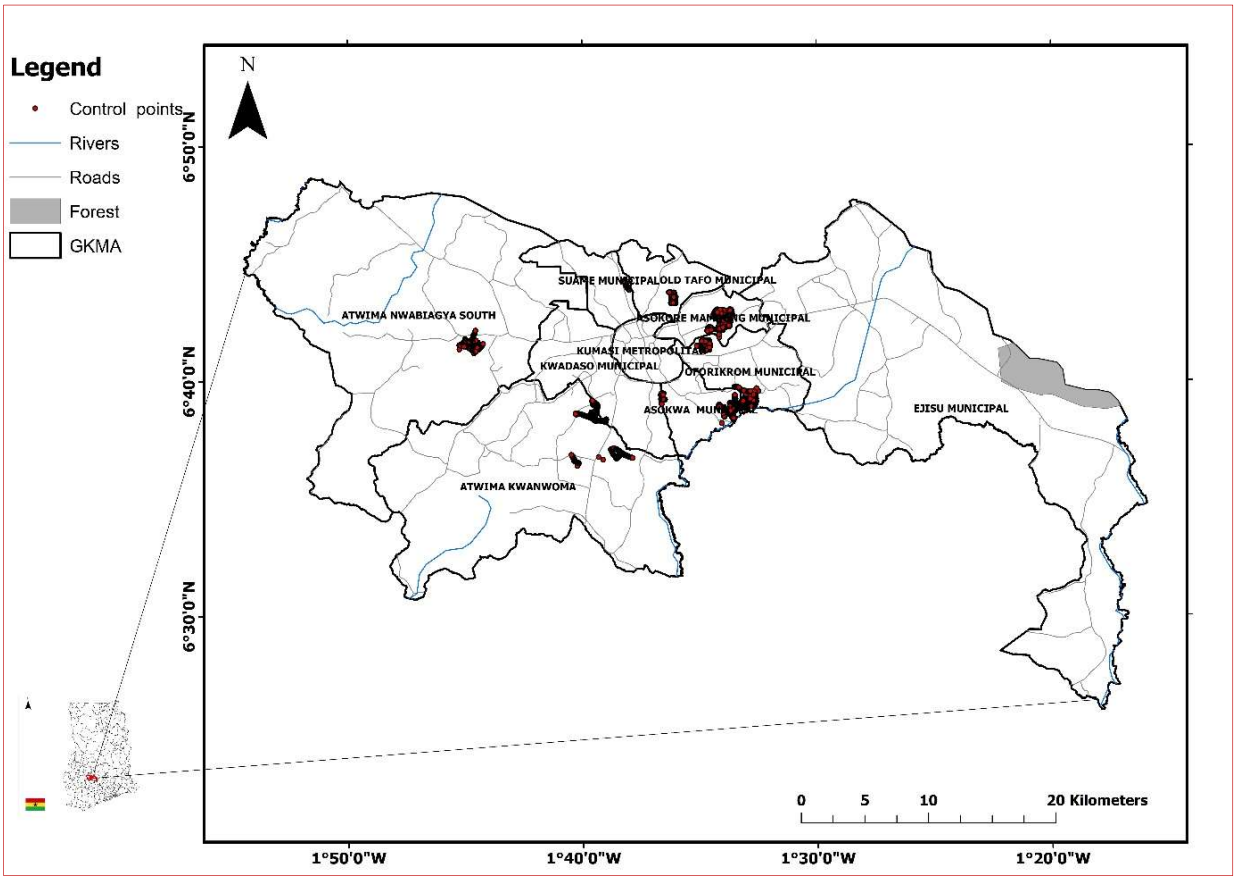

Fig. 1. Map of the study area

The applied methods estimated only horizontal positions and orthometric heights which were determined through levelling for the geodetic network. In view of that, several scholars have proposed different methodologies to aid in predicting ellipsoidal heights at a good precision. However, since classical methods cannot fully satisfy the current precision needs, it calls for the adoption of a more advanced prediction techniques, nevertheless, it needs to be studied and analyzed for comparable accuracies (Lee et al., 2020).

Commonly used methods for determining and predicting ellipsoidal heights includes levelling, contouring, least squares collocation, polynomial regression, Earth Gravitational Model and kriging. The levelling techniques is quite laborious, time consuming, expensive and requires rigorous field observations when large expanse of land is to be surveyed followed by post field computations (Ayer et al., 2016; Herbert and Ono, 2018; Peprah and Kumi, 2017). The process of extracting heights from contours on existing topographical maps and integrating with leveled spot heights can be problematic due to generalizations during contouring, and the need to interpolate between contours for specific grid nodes (Ayer et al., 2016). Hence, there is a necessity of utilizing some mathematical modeling techniques to eliminate discrepancies in the interpolation results (Ayer et al., 2016). The efficiency of Least Squares Collocation (LSC) for global and regional modelling do not hold without modifying the cross-variance function (Ophaug and Gerlach, 2017).

The Polynomial Regression Model (PRM) has a few problems associated with it. The best fit is obtained when the order is high(Chen and Hill, 2005; Tusat, 2011), but rather creates higher distortions when using the derived unknown

parameters (Poku-Gyamfi, 2009). Hence, there is the need to keep the order as low as possible. Increase in distance introduce noise and increase variance when using the kriging method (Erol and Celik, 2005). Earth Gravitational Model (EGM) accuracy cannot satisfy any civil engineering works (Al-Krargy et al., 2017) and its values needs to be validated using independent datasets (Abeho et al., 2014).

Despite the fact that these techniques have been utilized, they exhibit some practical drawbacks as have been elaborated by several scholars. In view of that, researchers have tried to evaluate the performance of Artificial Intelligence techniques for precise ellipsoidal heights predictions. Notably, the Artificial Neural Network (ANN) is one of the commonly used soft computing methods (Akyilmaz et al., 2009; Kaloop et al., 2017; Veronez, 2011).

El-Rabbany et al. (2015) conducted a comparative analysis between the developed neural network model and the sequential least squares method for tidal height prediction using tidal data series. It was revealed that the accuracy level of the tidal prediction improved by a factor of 5 when the neural network model was used. The ANN is computational models that imitate the human brain in performing a particular function through learning, or training, and then generalizing the network outputs for other inputs; A neural network consists of processing elements, or neurons, that are massively interconnected (El-Rabbany et al., 2015).

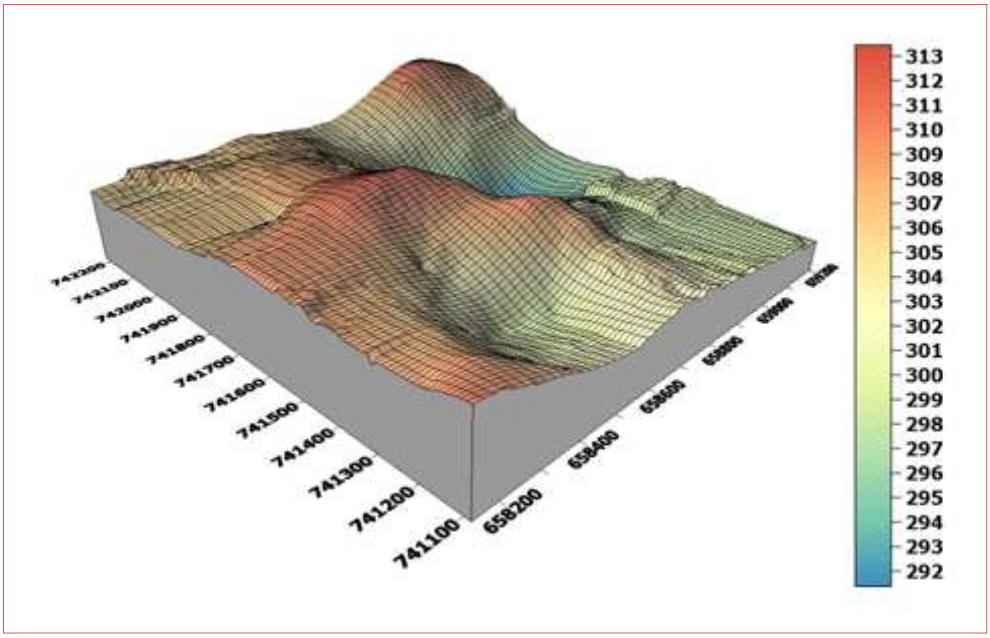

Fig. 2. 3D model map of study area

ANN has been successfully applied in heights predictions and datum transformation in Ghana (Peprah and Kumi, 2017). ANN techniques can be utilized in solving complicated problem (Kaloop et al., 2017). ANN techniques which is most widely used in geo-scientific discipline can form linear relationship between non-linear variables (Cakir and Konakoglu, 2019; Konakoglu, 2019).

The ANN has been used to solve some of the problems related to height issues in geodesy. Its suitability as an alternative technique to the classical methods of solving geodetic problems have been duly investigated (Yakubu and Dadzie, 2019). Notable among them are orthometric height predictions in a mine (Peprah and Kumi, 2017), GPS heights transformation (Fu and Liu, 2014; Liu et al., 2011; Wu et al., 2012; Yilmaz et al., 2017) and geoid modelling (Ahmadi et al., 2016; Akcin and Celik, 2013; Kao et al., 2017; Kavzoglu and Saka, 2005; Pikridas et al., 2011; Zaletnyik et al., 2007).

The authors concluded that, the results achieved by ANN models' techniques are encouraging and provides promising testaments in the future for solving some of the problems related to height issues (Akcin and Celik, 2013; Akyilmaz et al., 2009; Veronez et al., 2011). Conversely, other regressions algorithms have been developed and its efficacy in predicting heights are yet to be evaluated. For instance, GRNN have been used widely and yielded successfully results such as in coordinate transformation (Cakir and Konakoglu, 2019), predicting blast induced ground vibration (Arthur et al., 2019), and modelling data uncertainties (Yakubu and Dadzie, 2019).

In recent times, the efficiency of ARIMA, Polynomial Regression Model (PRM), and Multiple Linear Regression model (MLR) in solving majority of problems in geo-scientific community have been duly investigated as reported in (Peprah and Kumi, 2017; Yakubu et al., 2018). It is evident from related reviews and existing literatures that the applications of ANN techniques in Ghana are still limited and its suitability for ellipsoidal heights estimation for the study area has not been duly investigated. Hence, a comparison between these Artificial intelligence models and classical regression models have not been conducted. The existing knowledge and publications have not fully addressed

the issue of applying alternative techniques in predicting ellipsoidal heights in Ghana.

In addition, upon careful review of existing studies, the authors realized that the utilization of the BPANN, RBFANN, GRNN, ARIMA, PRM, and LSR techniques have not been applied as a practical alternative technology to the existing approaches in Ghana. This present study for the first time explored the utilization of the aforementioned techniques for the study area. To achieve the aim of this present study, all methods were applied. This study also highlights the comparison between ANN techniques to classical regression techniques. The statistical findings of these models will reveal their working efficiency and capabilities of the models for ellipsoidal heights determination. Hence this study will serve as an added contribution to existing knowledge of Artificial Intelligence and classical regression in mathematical geodesy. The purpose of this study is to propose a novel technique for ellipsoidal heights predictions and compare the model with classical regression techniques for the study area. The present study was conducted in the Greater Kumasi Metropolitan Assembly Local Geodetic Reference Network, Ghana which happens to be the study area.

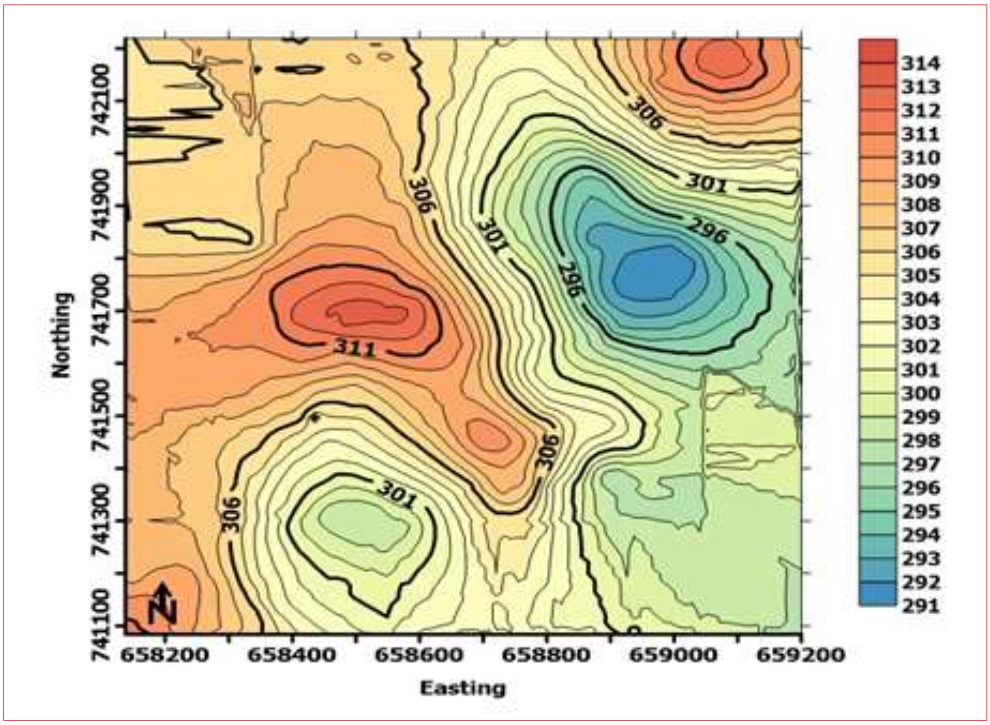

Fig. 3. Contour map of study area

This study for the first time in Ghana, applied and assess the performance of soft computing techniques and conventional techniques as an effective reliable tool for modelling ellipsoidal heights in the study area. Each model technique was assessed based on performance criteria indices such as *AME*, *AMSE*, minimum and maximum residual value, and *ASD*.

Also, the method of hypothesis testing (F and *t* Test) statistics was employed using the level of significance to determine the likelihood that a statement (often related to the mean or variance of a given distribution) is true or not (Massey snd Miller, 2004). This was done to verify whether there is a significant difference between the measured and predicted ellipsoidal heights, thereby testing the efficacy of the applied methods. This study will therefore create the opportunity for researchers in Ghana to know the performance of using soft computing techniques in solving some of the problems related to heights issues in the country. The authors were motivated to embark on this study since the aforementioned techniques is yet to be conducted in Ghana.

2. Resources and Methods Used

The GKMA is situated in the Ashanti Region, Ghana; comprises of the inner Kumasi and other neighboring municipalities and districts such as; Kwabre East, Afigya Kwabre Districts, Atwima Kwanwoma, Atwima Nwabiagya Districts, Asokore Mampong, Ejisu-Juaben and Bosomtwe District. It is geographically located between latitudes 6º 35`N and 6º 40`S and longitudes 1º 30`W and 1º 35`E with elevations ranging from about 250 to 350 meters above sea level (Acheamfour and Tetteh, 2014). It covers a total land area of 2,603km² with a total population of 3,190,473 (Oduro et al., 2014). The topography is undulating, traversed by a major river (Owabi) and streams like Subin, Wiwi, Sisai, Aboabo and Nsuben (Acheamfour and Tetteh, 2014; Atayi et al., 2018).

The horizontal geodetic datum of the study area is the War Office 1926 ellipsoid, and the vertical datum is the Mean Sea Level (MSL) which approximate the geoid (Peprah and Mensah, 2017) (Peprah and Kumi, 2017). The type of coordinate system used in the study area is Ghana projected

grid derived from the Transverse Mercator with 1° W Central Meridian and the World Geodetic System 1984 (WGS84) (UTM Zone 30N) (Yakubu et al., 2018). The Metropolis falls within the wet sub-equatorial type. The average minimum temperature is about 21.5 ºC and the maximum average temperature is about 30.7 ºC; the average humidity is around 84.16% at sunrise and 60% at sunset (Atayi et al., 2018).

The study area experience a double maxima rainfall regime which is about 214.3 mm in June and 165.2 mm in September (Acheamfour and Tetteh, 2014). The Metropolis lies in the transitional forest zone specifically within the moist semi-deciduous South-East Ecological Zone (Acheamfour and Tetteh, 2014). The study area is dominated by the middle Precambrian rock; two main lithostratigraphic/lithotectonic complexes, namely: the Paleoproterozoic supracrustal and intrusive rocks, and the Neoproterozoic to early Cambrian lithologically diverse platform sediments, exist in the study area; the unique geological structure has led to the development of the construction industry in the Metropolis with few small-scale mining activities and the proliferation of stone quarrying and sand winning Industries (Osei-Nuamah and Appiah-Adjei, 2017). Fig. 1 represents a map of the distribution of control points in the study area.

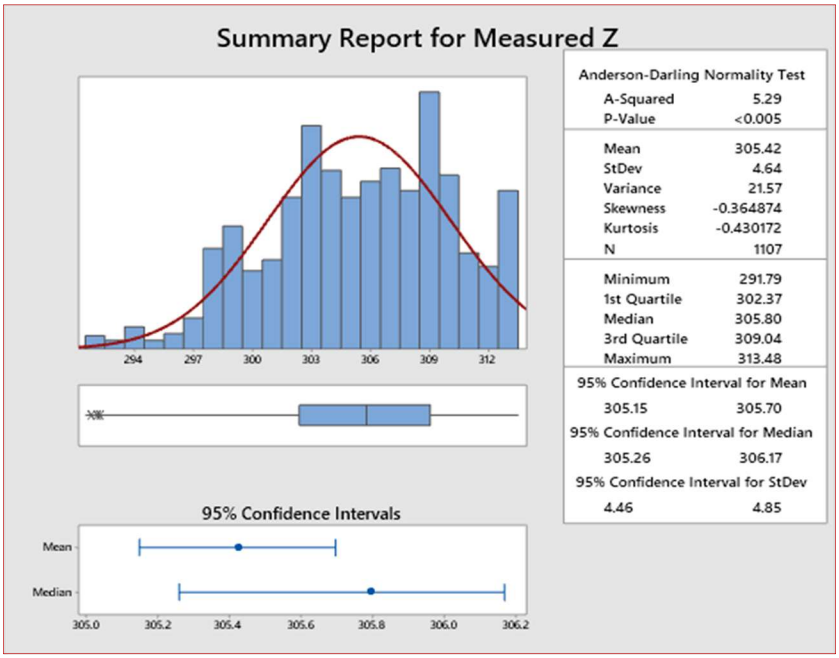

Fig. 4. Descriptive statistics of measured heights

Primary data used for the studies comprises of topographic data obtained from a survey in the Ghana urban water supply project in the GKMA. The sample data consists of 1107 control points collected with Real Time Kinematics (RTK) GPS instruments. The data comprise of three-dimensional coordinates namely eastings, northings, and ellipsoidal heights denoted as *(E, N, h)* were recorded using the RTK GPS instrument for the selected controls of the study area.

Figs. 2 and 3 depict the three-dimensional terrain model (3D) and contour map of the area respectively. Fig. 4 represents the summary report of the descriptive statistics of the GPS measured ellipsoidal height (*h*). Fig. 5 shows a structure of a modular neural network.

2.1. Methods

2.1.1. BPANN

BPANN is an effective multilayer perceptron (MLP) model (Yilmaz et al., 2017) and is widely used due to its simple implementation (Yakubu et al., 2018). BPANN consists of one input layer with M inputs, one hidden layer with q units and one output layer with n outputs (Mihalache, 2012). The M inputs in this study were the 3D coordinates $(N_{i,j}, E_{i,j}, H_{i,j})$, the q units were achieved by a trial and error training in changing number of hidden neurons, and the n outputs were the estimated ellipsoidal heights (h_i) achieved by the BPANN model. The output of the model (y_i) with a single output neuron is represented by *Equation 1* (Mihalache, 2012; Ziggah, 2017) as:

$$y(i) = f\left(\sum_{j=1}^{q} W_j f\left(\sum_{i=1}^{M} w_{j,i} x_i\right)\right) \quad (1)$$

where W_j is the weight between the hidden layer and the output layer, $w_{j,i}$ is the weight between the input layer and the hidden layer and x_i is the input parameter.

In this study, the selected input and output variables were normalized into the interval [-1, 1] using *Equation 2* given as (Mueller and Hemond, 2013):

$$Z(i) = \frac{y_{\min} + (y_{\max} - y_{\min}) \times (x_i - x_{\min})}{(x_{\max} - x_{\min})} \quad (2)$$

where $Z(i)$ represents the normalized data, x_i is the measured

coordinate values, while x_{min} and x_{max} represent the minimum and maximum value of the measured coordinates with y_{max} and y_{min} values set at 1 and -1, respectively.

The optimal model was obtained based on the lowest *AME*, *AMSE*, minimum residual error (r_{min}), maximum residual error (r_{max}) and *ASD*. Their mathematical expression is defined in model performance assessment section.

The present study adopted one hidden layer in the BPANN. This decision was in line with literature and conclusion made by Hornik et al. (1989) that the BPANN with one hidden layer could be used globally as an approximation for any discrete and continuous functions. Furthermore, to introduce non-linearity into the network, the hyperbolic tangent activation function was selected for the hidden units, while a linear function was applied for the output units. The hyperbolic tangent function is defined by *Equation 3* (Yonaba et al., 2010) as:

$$Z(x) = \tanh(x) = \frac{2}{1+e^{-2x}} - 1 \quad (3)$$

where; x is the sum of the weighted inputs.

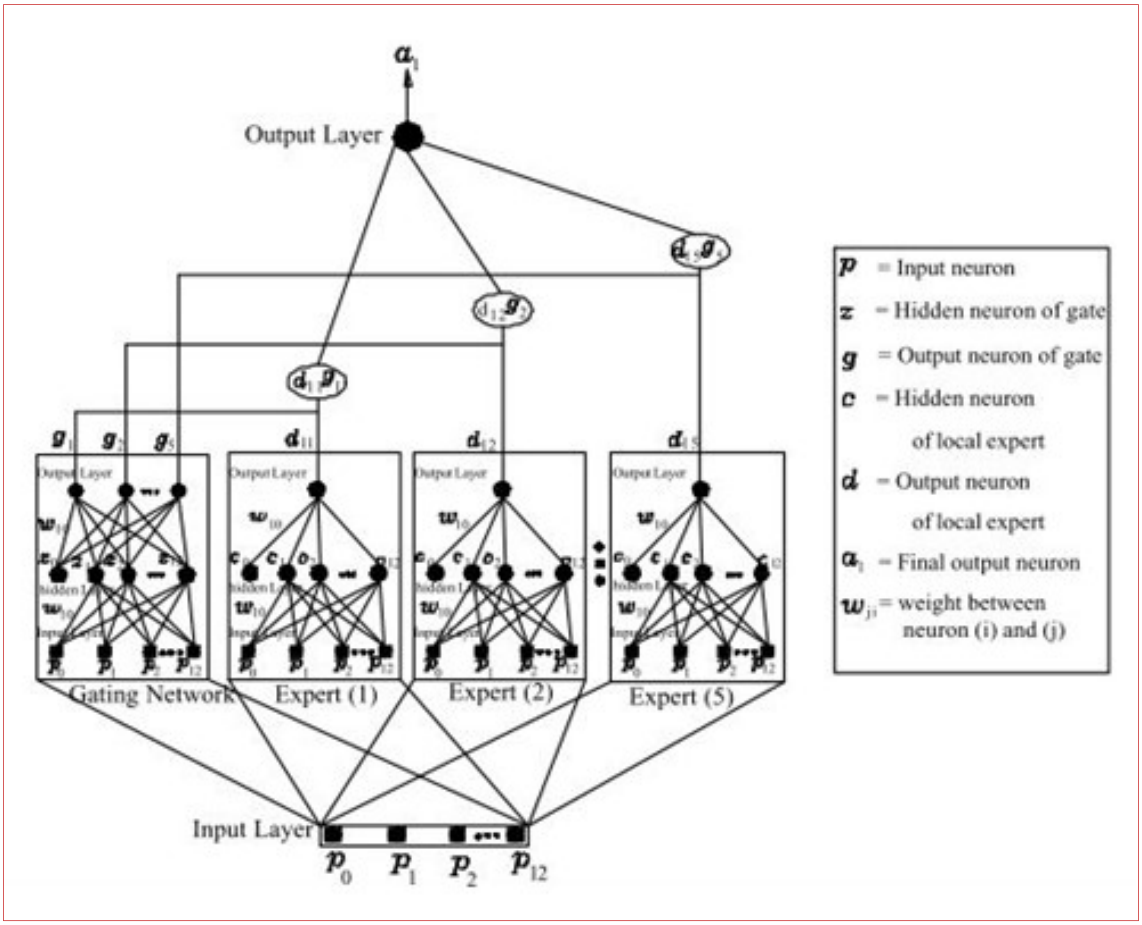

Fig. 5. A Structure of a modular neural network (El-Rabbany et al., 2015)

2.1.2. RBFANN

RBFANN model is an unsupervised learning algorithm which is constructed based on functional approximation. It consists of three functionally distinct layers namely; an input layer, a hidden layer and an output layer. The input layer is made up of sensory units that connect the network to its environment. In the second layer, the only hidden layer in the network applied a non-linear transformation from the input space to the hidden space.

The output layer is linear, supplying the response of the network to the activation pattern applied to the output layer. In this study, the input and output variables were the 3D coordinates denoted as (*N, E, h*) and (*h*) respectively. The dataset used for the formulation of the model were divided as training data which consist of 45 % of the total dataset and testing data which consists of 55 % of the total data set. RBFANN is an exact interpolator (Erdogan, 2009), hence a linear function is used in the input neurons and the connection between the input and hidden layers are not weighted (Kaloop et al., 2017). In this presented study, the Gaussian Function is applied, and the output neuron is a summation of the weighted hidden output layer given by *Equation 4* (Erdogan, 2009) as:

$$y(x) = \sum_{j=1}^{n} \kappa_j \chi_j(x) \quad (4)$$

where n is the number of hidden neurons, $x \in R^M$ is the input, $\kappa_j$are the output layer weights of the radial basis function network, $\chi_j(x)$ is Gaussian radial basis function given by *Equation 5* as (Idri et al., 2010; Srichandan, 2012):

$$\chi_j(x) = e\left(\frac{-\|x_i - c_j\|^2}{\sigma_j^2}\right) \quad (5)$$

where $c_j \in R^M$ and σ are the centre and width of jth hidden neurons respectively, $\|\ \|$ denotes the Euclidean distance.

2.1.3. GRNN

GRNN which was first introduced by Specht (1991) is a different kind of RBFANN, which is built on Kernel regression network (Hannan et al., 2010) with one pass learning algorithm and highly parallel structure (Dudek, 2011). GRNN consist of four layers namely; input layer, pattern layer (radial basis layer), summation layer, and output layer. In this study, the input variables (independent datasets) were the Northings, Eastings, and ellipsoidal height denoted as $(N_{i,j}, E_{i,j}, H_{i,j})$ and the output variables (dependent datasets) were the ellipsoidal height denoted as$(h_{i,j})$. The number of input units in the first layer depends on the total number of the observational parameters. The first layer is connected to the pattern layer and in this layer, each neuron is being presented by a training pattern and its output. The pattern layer is connected to the summation layer. The summation layer consists of two different types of summation namely, single division unit and summation unit (Hannan et al., 2010).

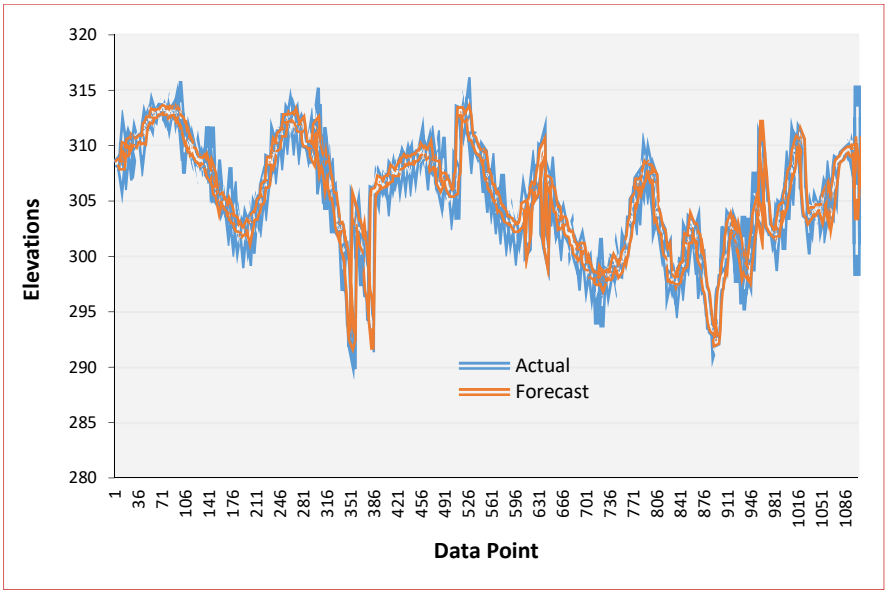

Fig. 6. Moving Average graph of ARIMA model

The summation with output layer combined perform a normalization of output datasets. In training of the network, radial basis and linear activation functions are used in hidden and output layers. Each pattern layer unit is connected to two neurons in the summation layer. One neuron unit computes the sum of the weighted response of the pattern, and the other neuron unit computes unweighted outputs of pattern neurons.

The output layer divides the output of each neuron unit by each other yielding the estimated output variables. In this present study, the Gaussian Function is applied, and the output neuron is a summation of the weighted hidden output layer given by *Equation 6* (Erdogan, 2009) as:

$$y(x) = \sum_{j=1}^{n} \kappa_j \chi_j(x) \quad (6)$$

where n is the number of hidden neurons, $x \in R^M$ is the input, $k_j$are the output layer weights of the radial basis function network, $\chi_j(x)$ is Gaussian radial basis function given by *Equation 7* as (Idri et al., 2010; Srichandan, 2012):

$$\chi_j(x) = e\left(\frac{-\|x_i - c_j\|^2}{\sigma_j^2}\right) \quad (7)$$

where $c_j \in R^M$ and σ are the centre and width of jth hidden neurons respectively, $\|\ \|$ denotes the Euclidean distance.

2.1.4. PRM

In this study, a polynomial mathematical model was adopted to model and predict the ellipsoidal height values. The horizontal coordinates (*N, E*) was used as the independent variables. The general expression of an *m*-degree polynomial interpolation is given by *Equation 8* denoted as (Yilmaz et al., 2017):

$$Z(N,E) = \Sigma_{i=0}^{m} \Sigma_{j=0}^{m-1} a_{ij} N^i E^j \quad (8)$$

where $Z_{(N,E)}$ is the ellipsoidal height information of the point with known horizontal coordinates (N, E) and $a_{i,j}$ is the unknown polynomial coefficients to be estimated, $(i,j = 0,\dots,m)$. The Simple Planar (SP) polynomial model was adopted in this study due to its efficiency and performance in estimating local heights as recommended by (Dawod et al., 2022; Peprah and Kumi, 2017). The general SP polynomial model is denoted by *Equation 9* given as:

$$Z_{ij} = a_o + a_1 N + a_2 E \quad (9)$$

where; Z_{ij} is the estimated ellipsoidal heights, (N,E) are the horizontal coordinates of the stationary positions, $a_{i,j}$ are the unknown parameters that can be determined using least square approach.

2.1.5. ARIMA

The ARIMA model introduce by Box and Jenkins (1976) is widely applied in time series forecasting. This type of model is a hybridized model which consists of autoregressive (AR) and moving average (MA), respectively (Yakubu et al., 2018). In ARIMA (p, d, q) modelling, the first step is to check the stationarity of the time series data. When the used time series data is not stationary, it has to be transformed into a stationary time series by applying the appropriate order of differencing d. The desired values of AR order p and MA q is acquired by checking the autocorrelation function and partial autocorrelation function of the time series data (Yusof et al., 2013). The AR (p) model is a discrete time linear equation with noise as expressed by *Equation 10* given as (Yakubu et al., 2018): Fig. 6 depicts the moving average graph of the ARIMA model.

$$\chi_t = \alpha_1 \chi_{t-1} + \cdots + \alpha_p \chi_{t-p} + \xi_t \quad (10)$$

where χ_t is the current forecasted model, p is the order, $\alpha_1, \cdots, \alpha_p$ are the parameters of coefficients of the model formed, χ_{t-1}, χ_{t-p} are the previous observations, and ξ_t is the error of the forecast.

The MA (q) model is an explicit formula for χ_t in terms of noise as given by *Equation 11*:

$$\chi_t = \xi_t - \beta_1 \xi_{t-1} - \cdots - \beta_p \xi_{t-p} \quad (11)$$

The difference operator Δ is given by *Equation 12*:

$$\Delta \chi_t = \chi_t - \chi_{t-1} = (1 - L)\chi_t \quad (12)$$

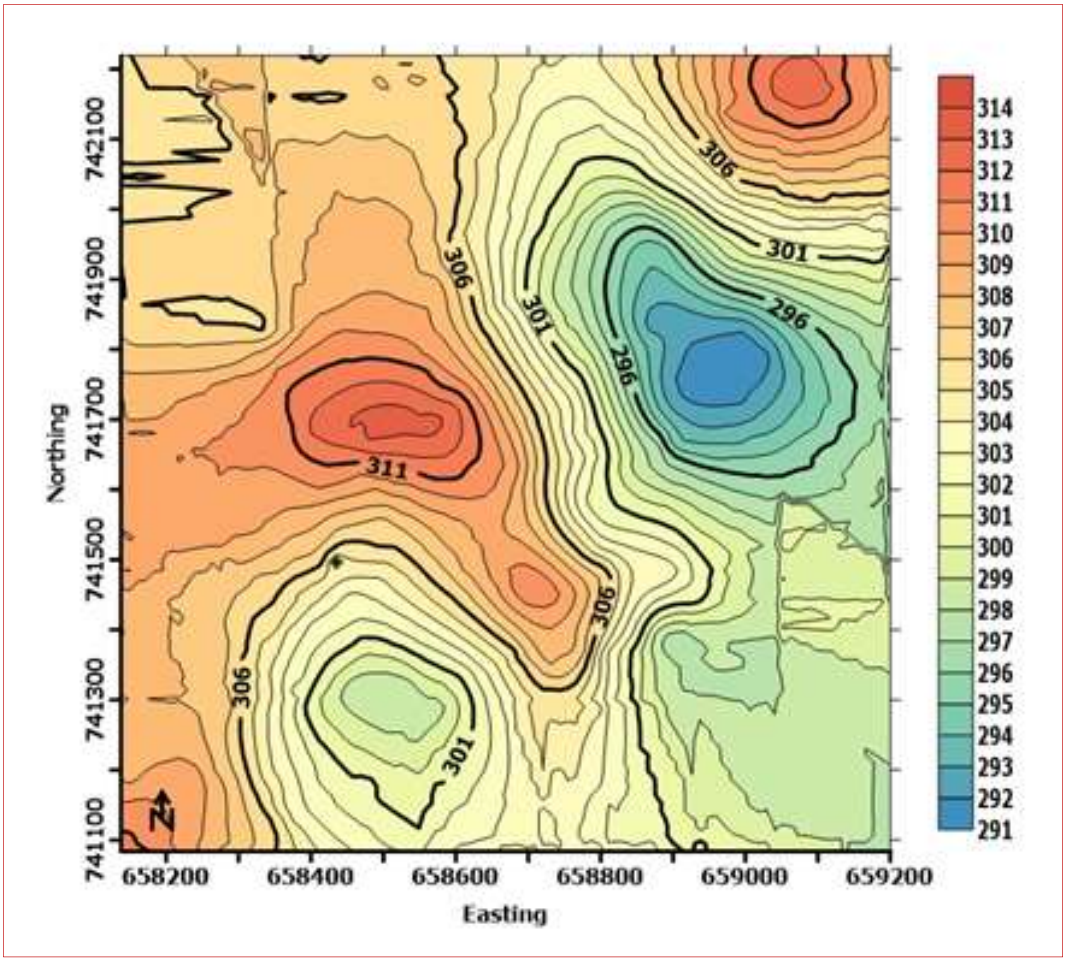

Fig, 7. RBFANN Contour map of the area

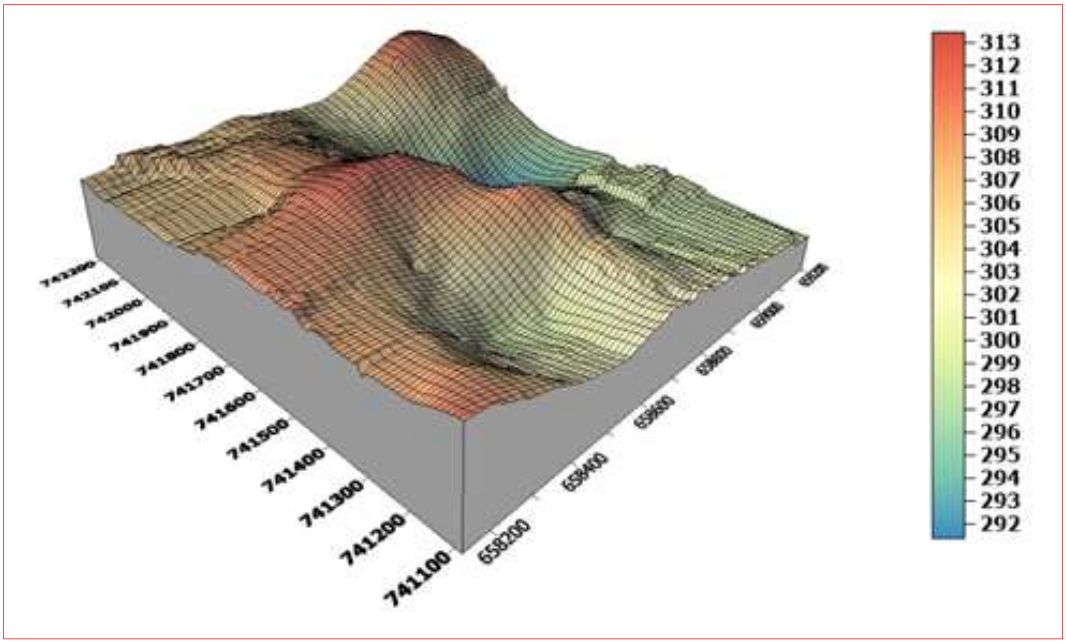

Fig. 8. RBFANN 3D Surface model of the area

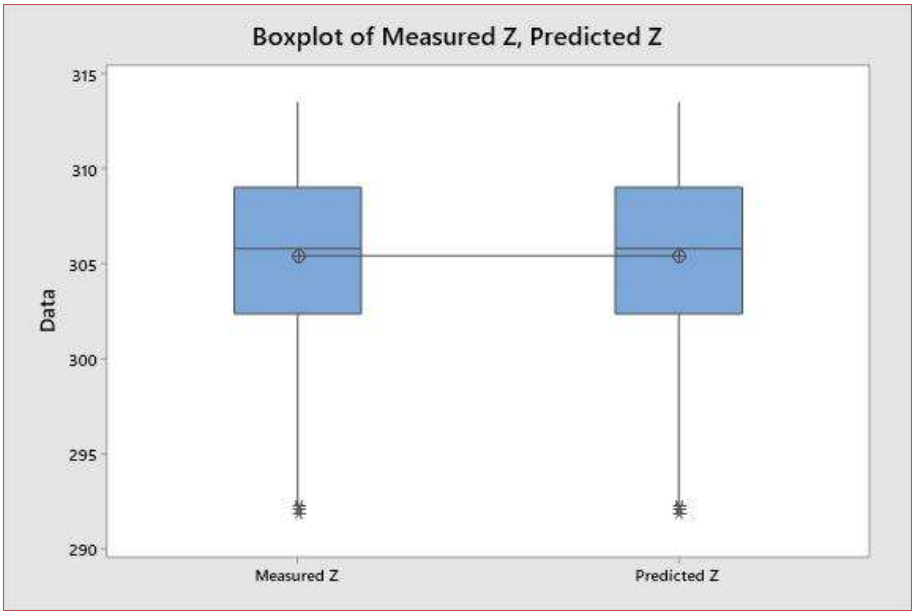

Fig. 9. Box plot statistics on RBFANN model

The ARIMA model with orders (*p, d, q*) is given by *Equation 13* as:

$$\left(1-\sum_{j=1}^{p}\alpha_j L^j\right)(1-L)^d \chi_t = \left(1+\sum_{j=1}^{q}\beta_j L^j\right)\xi_t \quad (13)$$

where L^j is the time lag operator, ξ_t is an error term, and d_i is the order of integration.

2.1.6. LSR

LSR method is a statistical technique that is capable of determining the line of best fit of a model and seeks to find the minimum sum of the squares of residuals. This method is extensively used in regression analysis and estimation (Miller, 2006; Peprah and Mensah, 2017). Considering a system of equations in the form as denoted by *Equation 14* to be solved by least squares:

$$DZ \approx L \quad (14)$$

where; $D \in R^{m\times n}$, $X \in R^{n\times d}$, $L \in R^{m\times d}$, $m \geq n$ (Annan et al., 2016; Schaffrin, 2006). D is the design matrix, Z is the matrix of the unknown parameters and L is the observation matrix. The solution of the unknown parameters matrix Z by ordinary least square approach can be achieved as denoted by *Equation 15*:

$$Z = [D^T D]^{-1}[D^T L] \quad (15)$$

The corresponding error vector V can be achieved by using *Equation 16*:

$$V = DZ - L \tag{16}$$

2.2. Model performance assessment

In order to determine the accuracies of the models being used, statistical error analysis was carried out. The statistical indicators applied were the *AME*, *AMSE*, r_{min} *and* r_{max} and *ASD*. Their mathematical expressions are given by *Equation 17* to *Equation 21* respectively as:

$$AME = \frac{1}{n}\sum_{i=1}^{n}(\alpha_i - \beta_i) \tag{17}$$

$$AMSE = \frac{1}{n}\sum_{i=1}^{m}(\alpha_i - \beta_i)^2 \tag{18}$$

$$r_{\max} = \alpha_i - \beta_i \tag{19}$$

$$r_{\min} = \alpha_i - \beta_i \tag{20}$$

$$ASD = \sqrt{\frac{1}{n-1}\sum_{i=1}^{n}(\mu - \bar{\mu})^2} \tag{21}$$

where, n is the total number of the observations, α_i and β_i are the measured and predicted ellipsoidal heights from the various techniques, μ denote the residual between the measured and estimated ellipsoidal height, $\bar{\mu}$ is the mean of the residual and i is an integer varying from 1 to n.

2.3. Hypothesis testing (F, t Test)

The method of hypothesis testing employs tests of significance to determine the likelihood that a statement (often related to the mean or variance of a given distribution) is true, and at what instance will statisticians accept the statement as true (Massey and Miller, 2004). F statistics refers to the ratio between the variances or mean squares of two independent data sets (Kumar Singh, 2015). The purpose is to determine whether there is a significant difference between the variances or precision of the data (Sureiman and Mangera, 2020).

A t Test is a parametric test that is used to compare the means of two groups (Kim, 2015). The reason is to verify whether there is a significant difference between the means of independent sample data (Ugoni and Walker, 2014).

Also, according to the central limit theorem, the means of a random sample of size, n, from a population with mean, μ, and variance, σ^2, distribute normally with mean, μ and variance, σ^2/n (Kwak and Kim, 2017). Hence, the parametric test can be applied on the large data sample ($n > 30$). Using α = 0.05 as the significance level (Massey and Miller, 2004), the hypothesis test can be expressed as;

$$H_O = S_a^2 - S_b^2;\ \mu_a - \mu_b = 0 \tag{22}$$

$$H_A = S_a^2 \neq S_b^2;\ \mu_a \neq \mu_b \tag{23}$$

where; H_O is the null hypothesis; H_A is the alternative hypothesis.

The test of significance using F test is denoted by (Kumar Singh, 2015);

$$F = \frac{S_a^2}{S_b^2},\quad S_a^2 = \frac{\sum\left(z_i - \bar{z}\right)^2}{n_a - 1} \text{ and } S_b^2 = \frac{\sum\left(z_i - \bar{z}\right)^2}{n_b - 1} \tag{24}$$

Under the assumption that the two samples display a normal distribution and have an equal variance (Kim, 2015; Massey and Miller, 2004), the t statistic is as follows:

$$t = \left[\frac{\left(\bar{z}_a - \bar{z}_b\right) - \left(\mu_a - \mu_b\right)}{S_p\sqrt{\frac{1}{n_a} + \frac{1}{n_b}}}\right] \tag{25}$$

where;

$$S_P^2 = \frac{(n_a - 1)S_a^2 + (n_b - 1)S_b^2}{n_a + n_b - 2} \tag{26}$$

where; $S_a^2 > S_b^2$; S_a^2 and S_b^2 are the respective variances of the first and second samples; μ_a and μ_b are the respective means of the first and second samples; Z_i is the value of an observation or measured value; $\bar{z}$ is the mean value of all observations, $\bar{z}_a$and $\bar{z}_b$are the first and second sample data; n is the number of observations; (n_a-1) and (n_b-1) are the degrees of freedom of the larger and smaller variance respectively.

In a two-tailed hypothesis test (Massey and Miller, 2004), the critical region is defined as;

$$|F| \geq F_{\alpha/2},n_a + n_b - 2;|t| \geq t_{\alpha/2},n_a + n_b - 2 \tag{27}$$

3 Results and Discussions

3.1 Developing of ANN models

A single layer BPANN model was trained using Bayesian Regularization (BR) learning algorithm. Tansig and Purelin functions were both used for the hidden and output layer when training BPANN model with BR respectively.

The optimal model structure, which is highly dependent on the number of hidden neurons was achieved through a sequential trial and error approach based on the lowest *AME*, *AMSE*, r_{max}, r_{min}, and *ASD*.

In this present study, the model was trained varying the number of hidden neurons from 1 to 50. The network was allowed to train for 1000 epochs with a learning rate of 0.03, and momentum coefficient of 0.7 for each iterative training process.

In the case of GRNN and RBFANN model training, both models' output is highly based on the value of the width

parameter (spread constant). Therefore, the optimal width parameter value for GRNN and RBFANN were also achieved based on a sequential trial and error approach for each iterative training process. Moreover, a gradient descent rule was implemented to train both GRNN and RBFANN models.

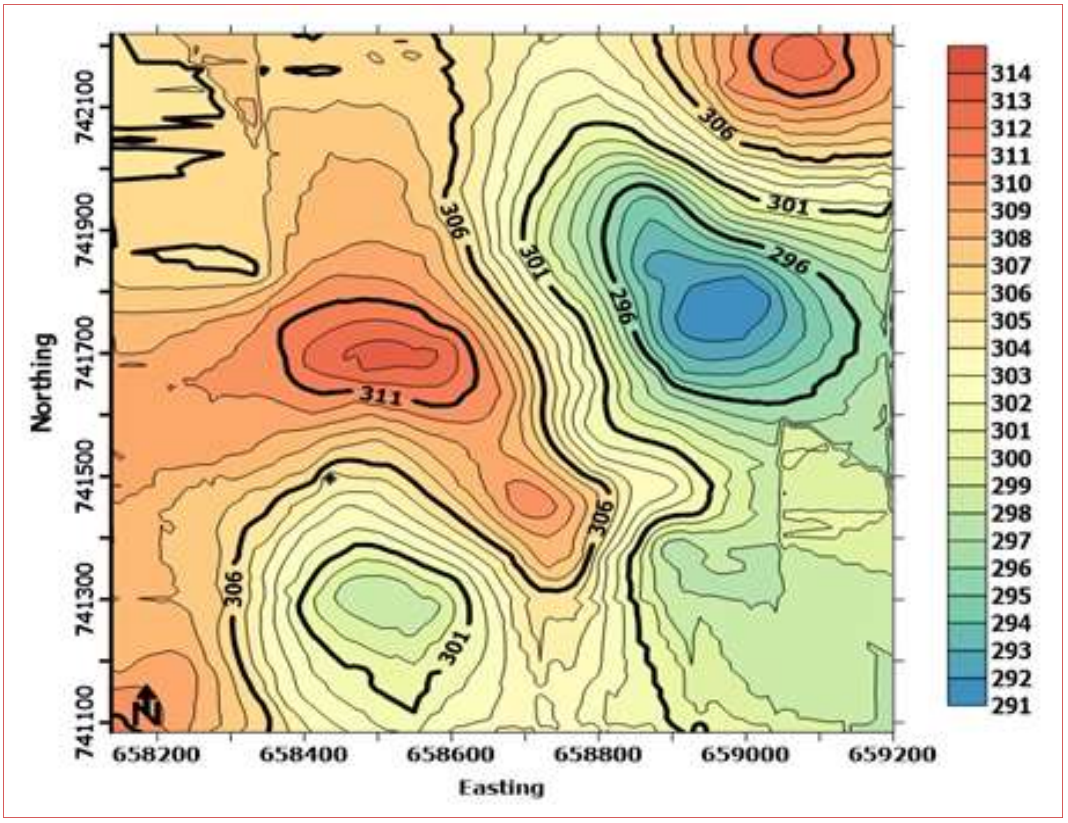

Fig. 10. BPANN Contour map of the area

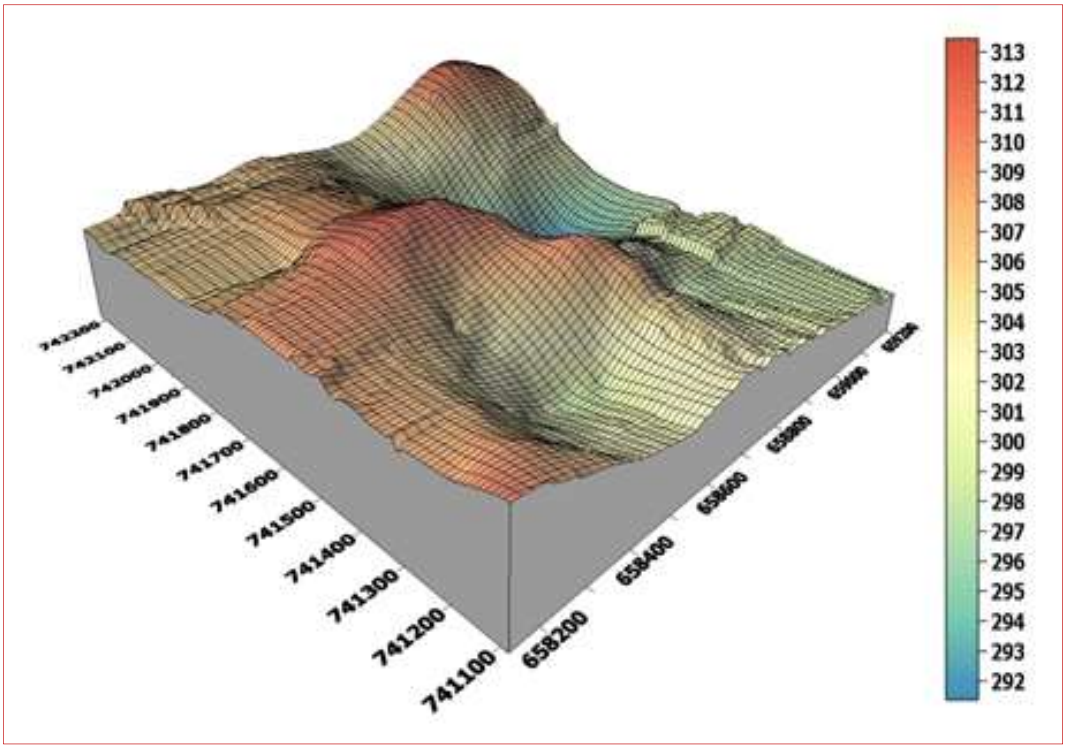

Fig. 11. BPANN 3D Surface model of the area

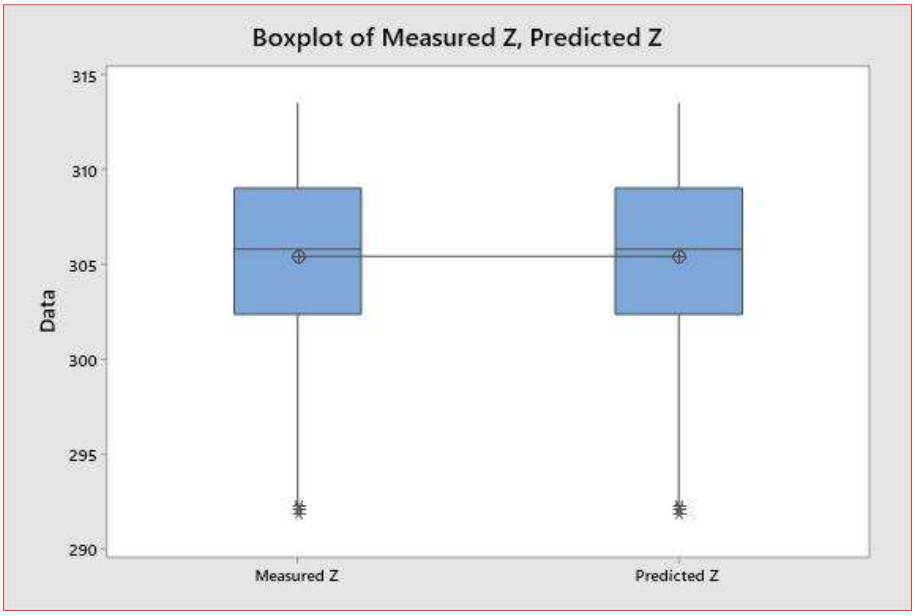

Fig. 12. Box plot statistics on BPANN model

The ANN models (BPANN, GRNN, and RBFANN) were coded and implemented in MATLAB (R2014a) software. After several trial and error method, the optimal model achieved by the BPANN model after successive iterative training was [3 10 1] thus, 3 input variables (independent dataset), 10 hidden neurons and 1 output variable (dependent dataset). Moreover, the optimal GRNN predictive model with the least statistical assessment values had a spread parameter of 0.9. This was achieved by varying the spread parameter (from 0 to 1) in each iterating training until the best results was achieved. Also, this implies that, the best optimal model achieved by the GRNN model is [3 0.9 1]. Thus, 3 input variables (independent variables), a spread constant of 0.9, and 1 output (dependent variables).

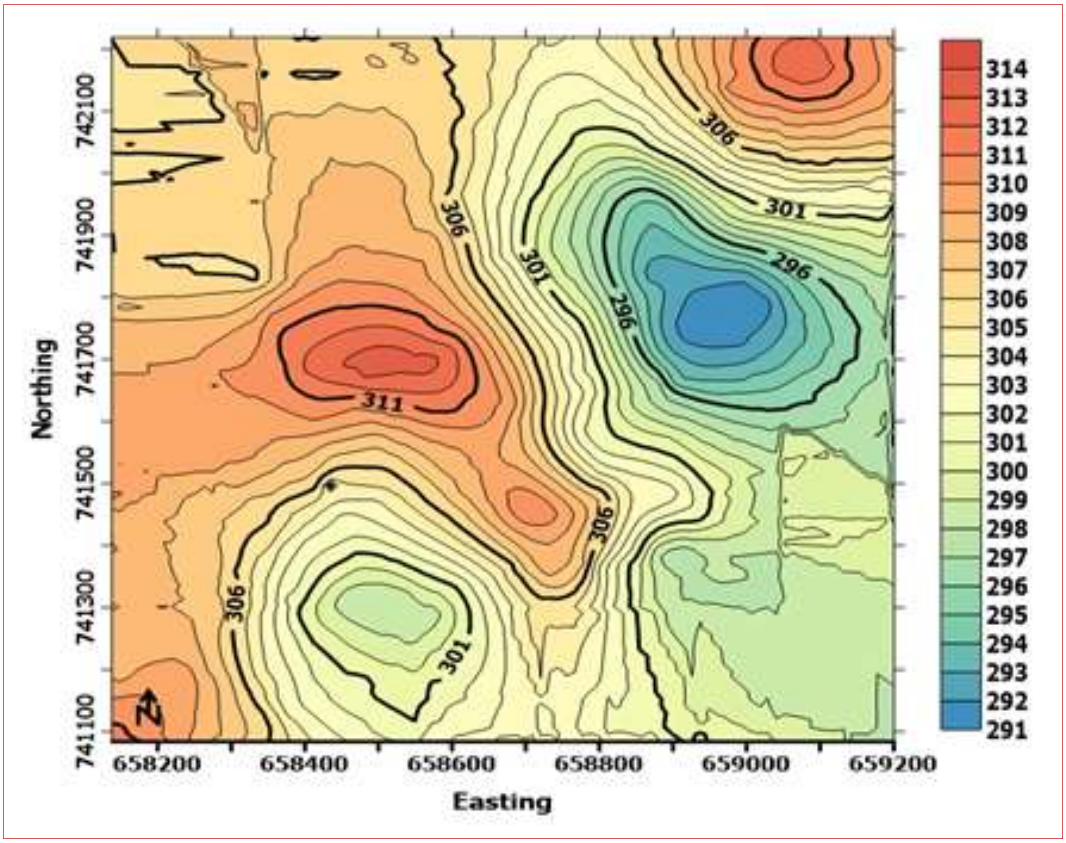

Fig. 13. GRNN Contour map of area

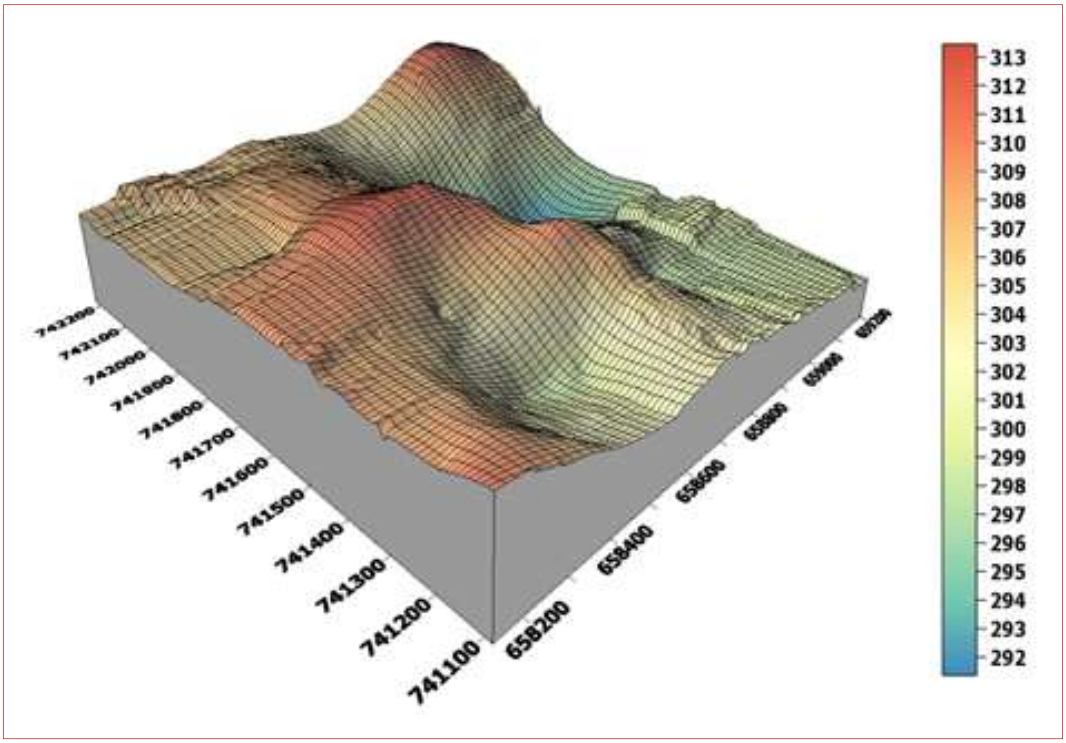

Fig. 14. GRNN 3D Surface model of area

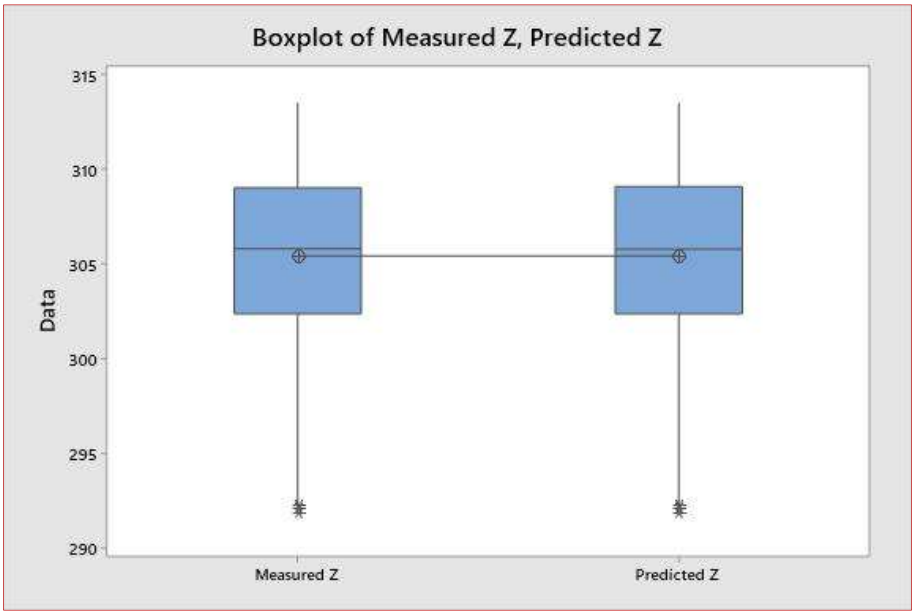

Fig. 15. Box plot statistics on GRNN model

The optimal RBFANN was achieved by varying the spread parameter (from 0 to 1) in each iterating training until the best results was achieved. Also, this implies that, the best optimal model achieved by the RBFANN model is [3 0.9 1]. Thus, 3 input variables (independent variables), a spread constant of 0.9, and 1 output dependent variable. This optimal RBFANN model structure gave the lowest minimum value in terms of their statistical analysis (lowest *AME*, lowest *AMSE*, and lowest *ASD*).

Figs. 7, 8, 10, 11, 13 and 14 show the contour map and 3D surface model of the study area achieved by the ANN models (BPANN, RBFANN, and GRNN) respectively. The figures shown revealed the superiority of the models in estimating local ellipsoidal heights when validated with the actual existing model (Figs. 2 and 3). All the ANN models (BPANN, RBFANN, and GRNN) truly represent the surface model of the area. The summarized results of the training and testing by all the soft computing techniques is represented by the Table 1. Based on the statistical results tabulated in Table 1, it can be observed that soft computing techniques provide satisfactory results in estimating local ellipsoidal heights with

much better accuracy for the study area. The minimum and maximum residuals are very quiet encouraging. The arithmetic mean error (*AME*), arithmetic mean square error (*AMSE*), and arithmetic standard deviation (*ASD*) of both training and testing are quite good and very much encouraging. However, ANN has proven to be a powerful realistic alternative tool in computing local ellipsoidal heights for the study area with much better accuracy.

Table 1. Model results for Soft Computing Techniques (units in meters)

Training Results			
PCI	**GRNN**	**BPANN**	**RBFANN**
r_{max}	0.1905	8.3478×10^{-04}	4.0359×10^{-12}
r_{min}	-0.4539	-1.2299×10^{-03}	-5.9686×10^{-12}
AME	6.9761×10^{-04}	-6.3820×10^{-07}	-4.1496×10^{-14}
AMSE	2.4333×10^{-04}	2.0365×10^{-10}	8.6095×10^{-25}
ASD	0.1087	2.0424×10^{-04}	6.2690×10^{-13}
Testing Results			
PCI	**GRNN**	**BPANN**	**RBFANN**
r_{max}	0.5327	6.1589×10^{-04}	3.0127×10^{-12}
r_{min}	-0.5967	-1.2215×10^{-04}	-1.0232×10^{-12}
AME	-9.4249×10^{-04}	-3.3938×10^{-06}	3.9828×10^{-14}
AMSE	5.4249×10^{-04}	6.9914×10^{-09}	9.6603×10^{-25}
ASD	0.1131	1.8962×10^{-04}	3.5547×10^{-13}

Table 2. Least Square Regression Coefficients Results (units in meters)

Coefficients	**Value**
a_0	7.03331×10^{02}
N_i	0.0078
E_i	0.0094

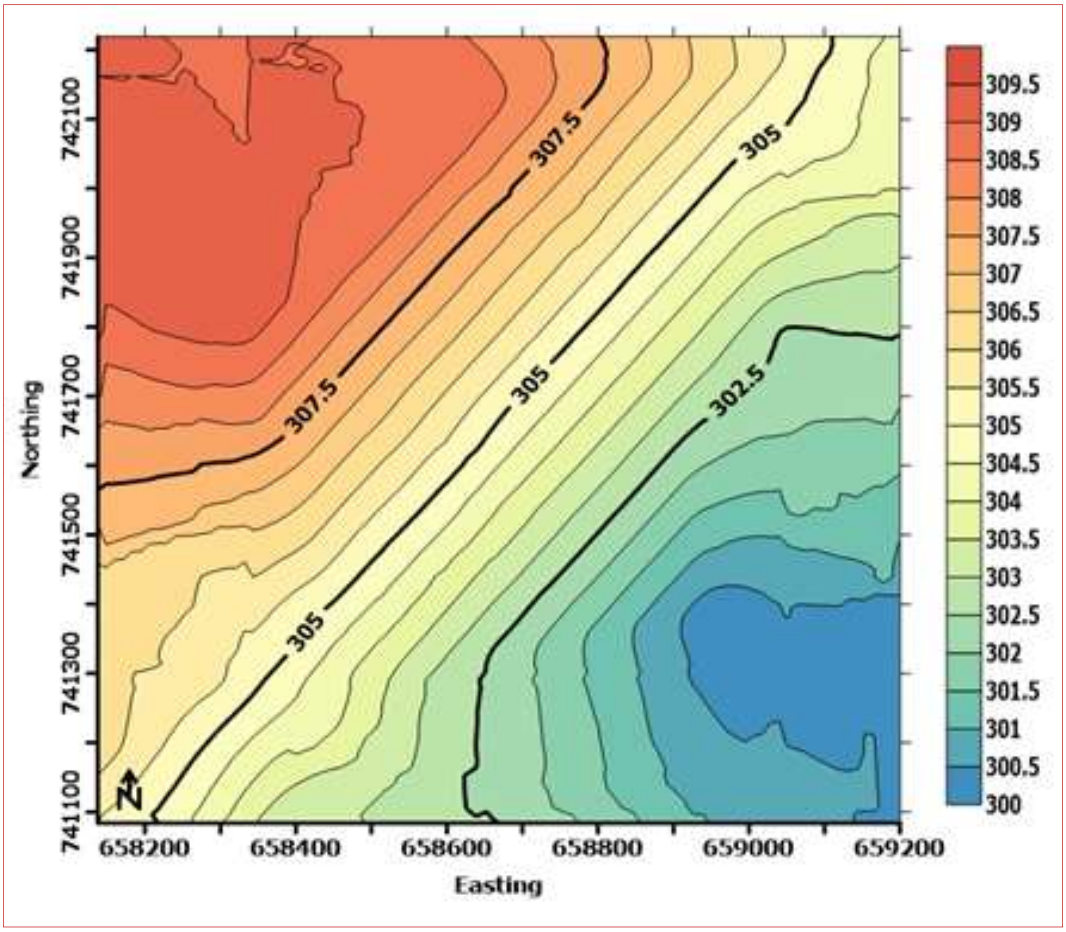

Fig. 16. PRM Contour map of area

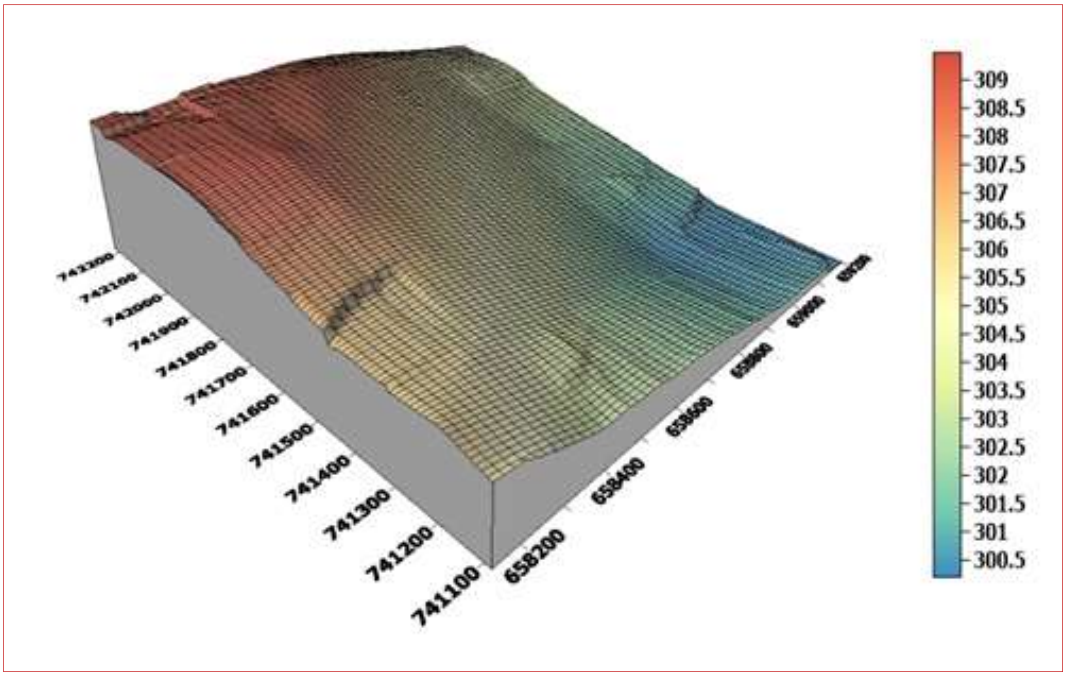

Fig. 17. PRM 3D Surface model of area

3.2. Developing the classical regression models

In formulating the PRM model, a statistical description of the data was performed by using the Minitab 19 software to find the correlation between the independent variables (input datasets) and the dependent dataset (output datasets). The optimal PRM equation generated by the Minitab software for estimating the ellipsoidal heights is given by *Equation 27* as:

$$Z(i) = 703 + (0.007839 \times N(i)) - (0.009431 \times E(i)) \quad (27)$$

where; *Z (i)* is the dependent variables (Ellipsoidal heights), {703, 0.007839, 0.009431} are the generated unknown parameters by the Minitab software. The final estimated *Z (i)* values with the given equation and parameters were coded and implemented in MATLAB environment. Moreover, in developing an optimal ARIMA model using the MATLAB software, non-stationarity which existed in the observed data which will results in wrong statistical inferences was resolved by differencing the data to ensure that the data is stationary.

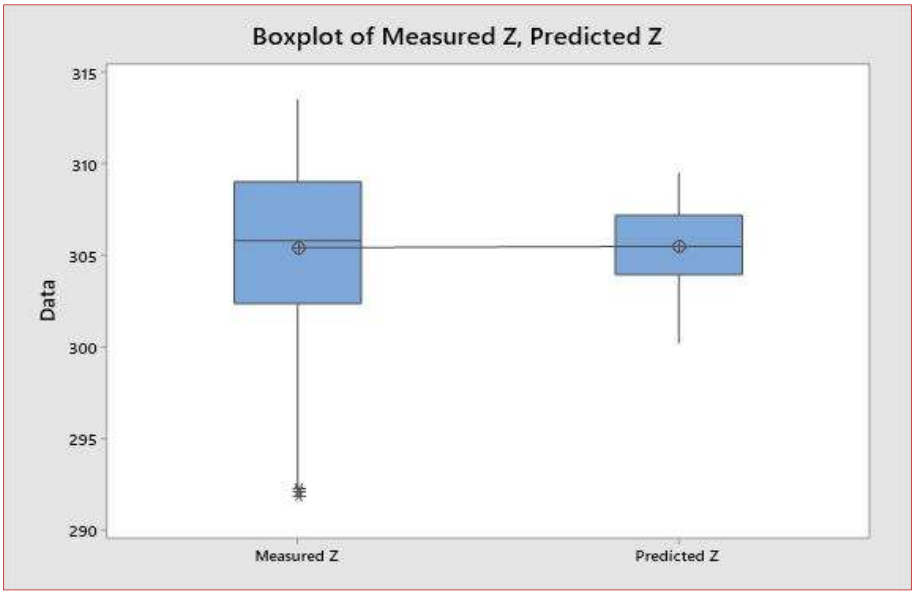

Fig. 18. Box plot statistics of PRM

In this study, ARIMA (0, 1, 1) model was the optimal model been developed from the observed stationary field data to predict the ellipsoidal heights for the study area. The solution to the least squares methods in estimating the unknown parameters of the LSR model was coded and implemented in MATLAB.

Table 2 is the estimated unknown parameters of the LSR model using the Minitab software. Figs. 16, 17, 19, 20, 22 and 23 are the contour map and 3D surface model by the classical regression (PRM, ARIMA and LSR) models respectively.

The figures revealed that, the ARIMA model compared to the PRM and LSR model shown superiority in predicting the local ellipsoidal heights for the study area when validated with the existing models (Figs. 3 and 4). The achieved results by the ARIMA model indicates the extent of agreement between the observational data points and models predicted values. Thus, the ARIMA model had a good fit to the observe data (Figs. 3 and 4) than PRM and LSR model.

On the basis of the results achieved in this present study, the classical ARIMA model outperformed the PRM and LSR model in predicting local ellipsoidal heights for the study area at the moment. Therefore, the inference made here is that, the ARIMA technique has demonstrated a better predictive performance and has a stronger efficiency in predictions of local ellipsoidal heights with the entire dataset than the PRM and LSR model.

In addition to that, the ARIMA being a hybrid model thus, consists of the *AR (p)* model and the *MA (q)* model uses both the strength and weakness of *AR (p)* and *MA (q)* to complement each other. Also, the model is able to combine the *AR (p)* and *MA (q)* function estimation and nonlinear modelling capabilities. The superiority of the ARIMA to PRM and LSR model was further demonstrated when comparison was made between their obtained *AME*, *AMSE*, r_{max}, r_{min} and *ASD*.

In Table 3, the ARIMA model achieved a promising result as compared to PRM and LSR. This implies that, the classical ARIMA model can predict accurately local ellipsoidal heights from the observed data for the study area than PRM and LSR model.

3.3. Comparing the predictive performance and hypothesis results of the ANN models with the classical models

BPANN predictive model with improved statistical metrics was observed at a structure of 3 inputs, a hidden layer with 10 neurons, and 1 output. While the GRNN predictive model structure was identified as 3 inputs, a width parameter of 0.9, and 1 output. Similarly, the optimal RBFANN was achieved by varying the spread parameter (from 0 to 1) in each iterating training until the best results was achieved. This implies that, the best optimal model achieved by the RBFANN model is [3 0.9 1]. Thus, 3 input variables (independent variables), a spread constant of 0.9, and 1 output dependent variable.

In the hidden layer chamber, the input layer data is received by means of connections that are not weighted. The data is then transformed by means of a non-linear activation function with each neuron estimating a Euclidean norm that depicts the distance between the inputs to the network. This is then inserted into a radial basis activation function which calculates and outputs the activation of the neuron (Kumi-Boateng and Ziggah, 2017).

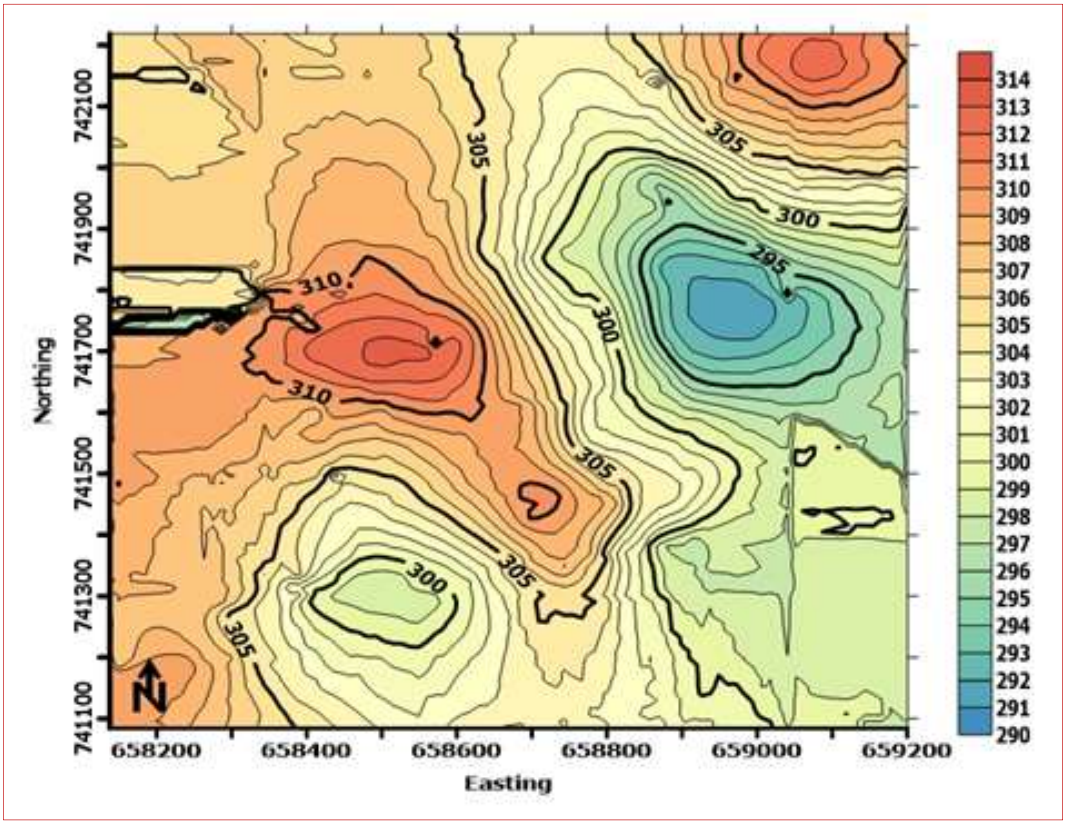

Fig. 19. ARIMA Contour map of the area

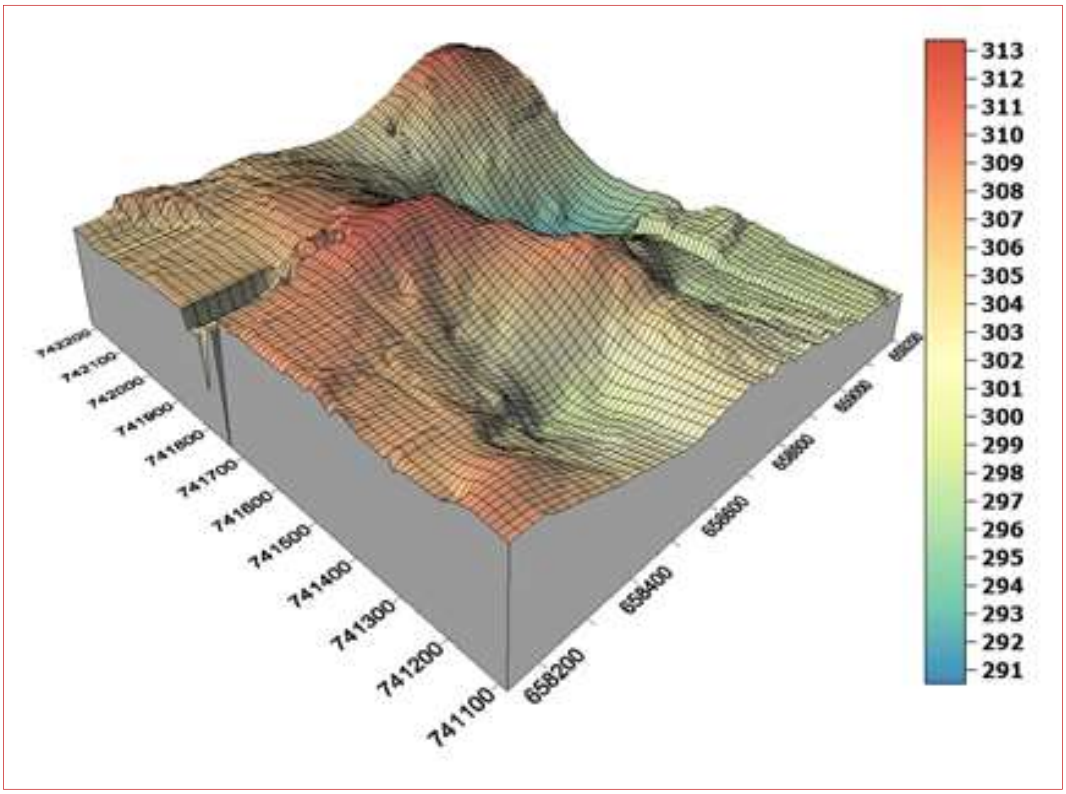

Fig. 20. ARIMA 3D Surface model of area

The Gaussian transfer function was used for the hidden layer of the RBFANN (Konakoglu, 2019). The optimal RBFANN model structure gave the lowest minimum value in terms of their statistical analysis (lowest *AME*, lowest *AMSE*, and lowest *ASD*). Also, the optimal ARIMA model achieved was (0 1 1). The soft computing techniques (BPANN, RBFANN, and GRNN) have been compared to the conventional techniques (PRM, ARIMA and LSR) using all the data points. The statistical analysis is represented by Table 3.

From Table 3, it is seen that the proposed ANN techniques similar satisfactory results as compared to the classical techniques. The reason is related to the reported statistical assessment. Statistical analysis of Table 3 indicates that the proposed ANN models' predictions were closely related to the observed ellipsoidal height with a higher prediction accuracy. The same was observed for the ARIMA model with a high prediction accuracy in estimating the observed ellipsoidal heights at a good precision.

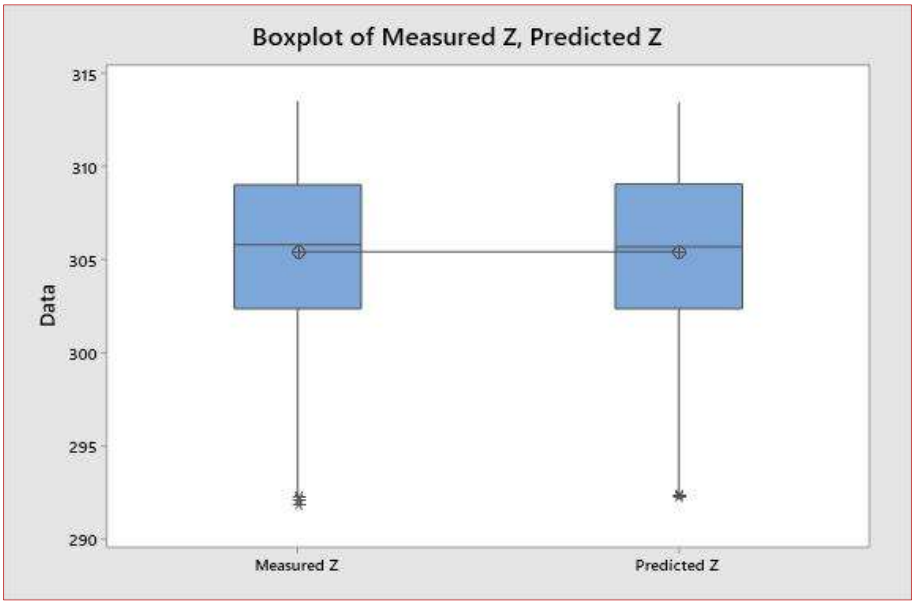

Fig. 21. Box plot statistics on ARIMA model

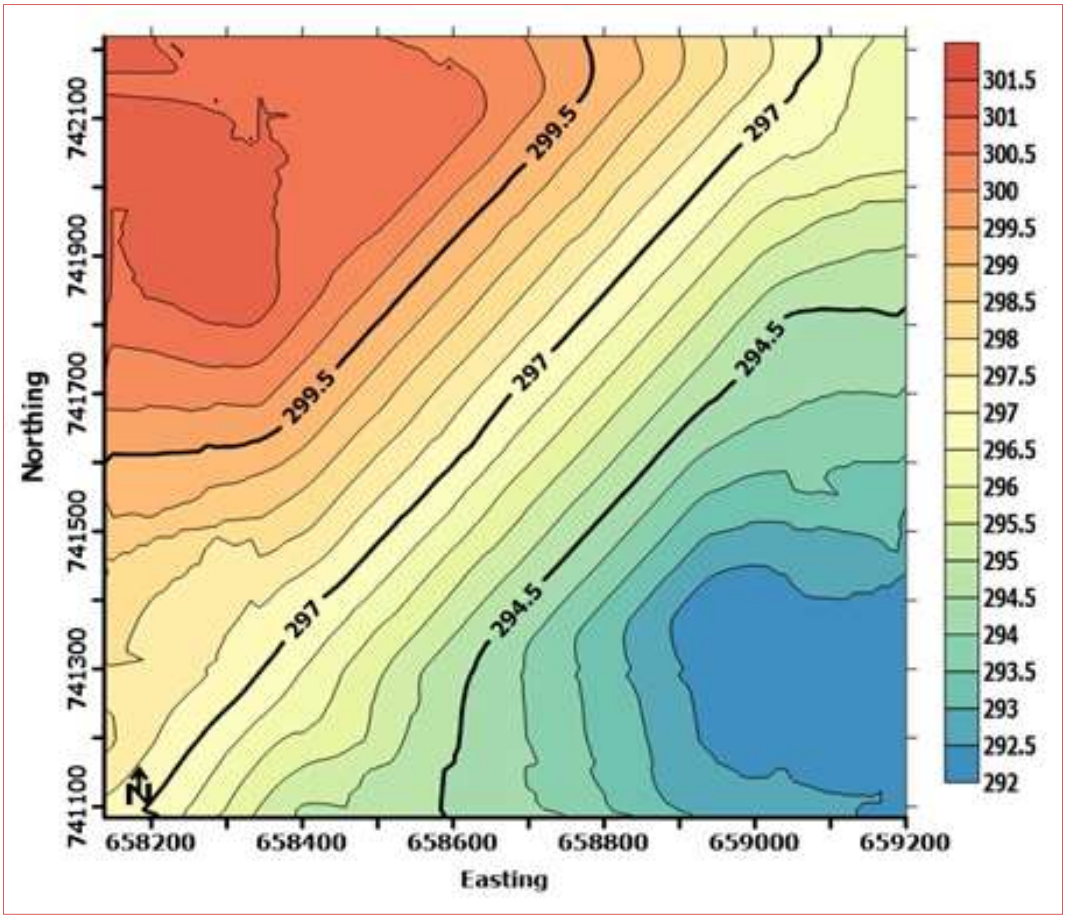

Fig. 22. LSR Contour map of area

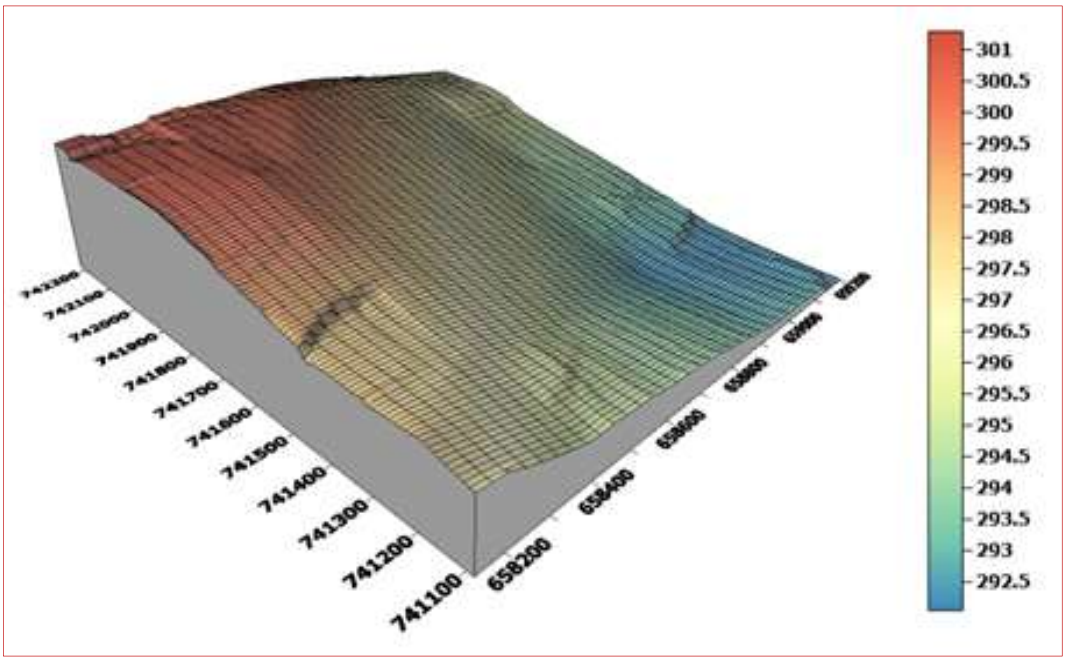

Fig. 23. LSR 3D Surface model of area

PRM and LSR models were observed to predict the ellipsoidal heights at a lesser accuracy. The maximum residual values of the conventional techniques and the soft computing techniques were 15.9312 m and 0.5327 m respectively. When comparing their statistical analysis, the PRM model had a minimum residual value of -12.2154 m and ASD of 4.0473 m. This situation agrees by the recommendation as represented by Chen and Hill (2005) and

Poku-Gyamfi (2009) that, the defects of the PRM model is due to the increase in order and there are distortions in the estimated values using the transformed parameters estimated by the least squares approach and the order must be kept low. The performance of the soft computing techniques outperforms the conventional techniques in estimating local ellipsoidal heights. Also, the lower performance of the classical techniques may be attributed to the unknown parameters used in the model in estimating the ellipsoidal height. After comparing the soft computing techniques to the conventional techniques in terms of their statistical analysis, the soft computing was much better as compared to the conventional methods in estimating local ellipsoidal heights for the study area. ARIMA model compared to PRM and LSR showed better performance in predicting the ellipsoidal heights for the study area.

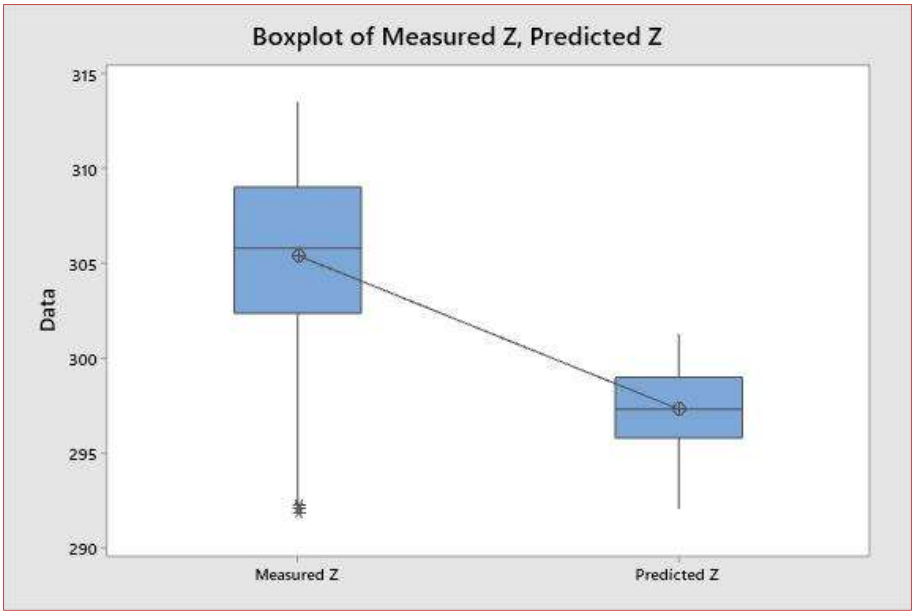

Fig. 24. Box plot statistics on LSR

Table 3. Statistical Analysis of all models (units in meters)

PCI	r_{max}	r_{min}	AME	AMSE
RBFANN	4.0359×10^{-12}	-5.9686×10^{-12}	3.1322×10^{-15}	1.0861×10^{-26}
BPANN	8.3478×10^{-04}	-1.2299×10^{-03}	-2.1492×10^{-06}	5.1132×10^{-09}
GRNN	0.5327	-0.5967	-2.033×10^{-04}	4.5746×10^{-05}
ARIMA	4.9013	-6.3007.	0.0012	0.0017
PRM	7.7487	-12.2154	-0.0764.	6.4550
LSR	15.9312	-4.0399	8.1007	7.2642×10^{03}

Fig. 25 and 26 shows the AMSE and ASD model graphs of all the applied techniques. The statistical hypothesis testing (F, *t* Test) employed in the study is given by *Equation 22* to *Equation 26*. This was carried out to determine whether there is a significant difference between the means and variances of the measured and predicted ellipsoidal heights to further validate the performance of the various models. The hypothetical statements are expressed by *Equation 22* and *23*. The F and *t* statistics is denoted by *Equation 24* and *25*, respectively.

The two-tailed critical region is shown by Equation 26. Table 4 displays the results of the statistical hypothesis testing showing the mean, variances, standard deviation, standard error means, Upper and Lower limits of the 95% Confidence Interval (CI), F, *t* and their P values.

From Table 4, the mean and variances of the predicted ellipsoidal heights using the ANN models (RBFANN, BPANN, and GRNN) are all equal to that of the measured or observed ellipsoidal heights. Hence, the need to conduct F and *t* Tests to verify whether there is truly no significant difference between their means and variances.

For the F statistics test, the P values obtained for the ANN models were greater than the level of significance ($p>0.05$). This implies their variances are equal or very similar to the measured ellipsoidal heights, and they have less than 95% confidence that there is a significant difference between their variances, hence the null hypothesis is accepted.

The order of similarity of the variances of the ANN models is depicted by; $P_{RBFAAN}>P_{BPAAN}>P_{GRNN}$ as displayed in Table 4. For the, *t* statistics test, the P values obtained for the ANN models were greater than the level of significance ($p>0.05$). This implies their means are equal or very similar to the measured ellipsoidal heights, and they have less than 95% confidence that there is a significant difference between their

means, so then the null hypothesis is accepted. Also, the order of similarity of the variances of the ANN models is depicted by; $P_{RBFAAN}>P_{BPAAN}>P_{GRNN}$ as displayed in Table 4. This can be seen by their mean and variability (upper quartile, lower quartile and Interquartile ranges) expressed by the comparative Box plots in Figs. 9, 12 and 15.

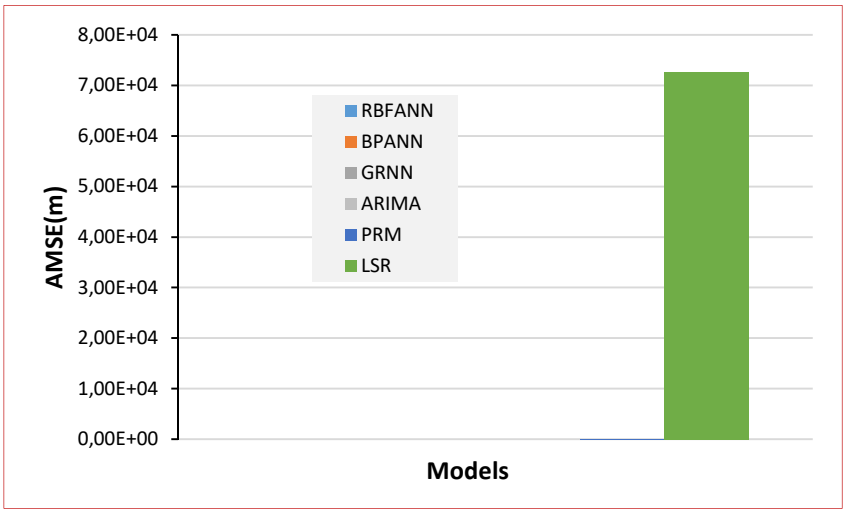

Fig. 25. AMSE Graph of the models

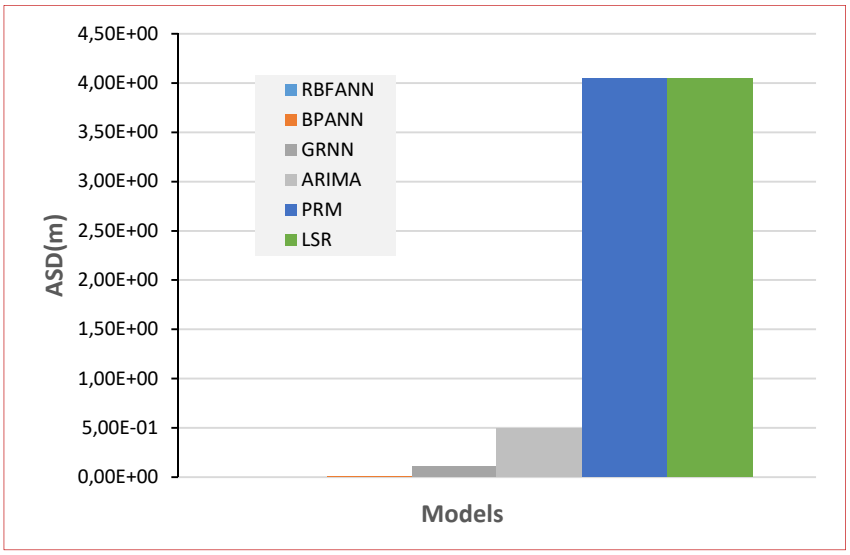

Fig. 26. ASD Graph of the models

Table 4. Hypothesis Testing of all models

	Independent samples test				95% CI		Test of significance, $(\alpha = 0.05)$			
Model	**Mean**	**Error mean**	**SD**	**Variance**	**Lower**	**Upper**	**F test**	**P (2-tailed)**	***t* Test**	**P (2-tailed)**
RBFANN	305.42	0.14	4.64	21.53	-0.387	0.387	1	1	0	1
BPANN	305.42	0.14	4.64	21.53	-0.387	0.387	1	0.9999	0	0.9999
GRNN	305.42	0.14	4.64	21.53	-0.387	0.387	1	0.9853	0	0.9514
ARIMA	305.42	0.14	4.60	21.16	-0.384	0.387	1.02	0.7538	0.01	0.933
PRM	305.50	0.068	2.28	5.20	-0.381	0.229	4.16	6.39×10^{-115}	-0.05	0.623
LSR	297.32	0.068	2.27	5.16	7.796	8.405	4.19	3.50×10^{-116}	52.15	0

From Table 4, the ARIMA model achieved the same mean as the observed ellipsoidal height but a slight difference in their variance. For confirmation, the F and *t* tests were performed; the achieved P value using the F statistics shows a similarity in variance with the measured ellipsoidal heights but is lower compared to those achieved by the ANN models. For the *t* Test, the achieved P values were also greater than the level of significance but lower than that of the ANN models, hence the null hypothesis was accepted for both tests. This can be seen in the Box plot shown by Fig. 21. The PRM

model achieved a similar mean but a lower variance compared to that of the observed ellipsoidal heights; the achieved P value using the F statistics shows a vast significant difference in variance with the measured ellipsoidal heights and the ANN models as seen in Table 4. Hence, the null hypothesis is rejected and the alternative hypothesis is accepted. In order to perform *t* Tests the condition of equal or similar variance needs to be satisfied (Kim, 2015).

The PRM model have unequal variance with the observed heights, but on the basis of assumption of equal variance the obtained P value using the *t* Test shows a similarity between the means ($p>0.05$) which is still lower than that of the ARIMA and ANN models; hence the null hypothesis is accepted. The mean and behavior of the variance of the PRM model is depicted by Fig. 18. Under the assumption that the two samples display a normal distribution and have an equal variance (Kim, 2015; Massey and Miller, 2004); the F and *t* Test were also performed on the LSR model.

From Table 4, the achieved means and variance of the LSR model were different from those of the observed ellipsoidal height; this was verified using the F and *t* statistics. The P values obtained using both test statistics shows a vast significant difference ($p<0.05$) between the means and variances of the LSR model and that of the observed height and ANN models; therefore, the null hypothesis is rejected and the alternative hypothesis is accepted. The mean and variability results of the LSR model is displayed in Fig. 24.

From Figs. 18 and 24, The average sample variability of the measured heights is higher than the average sample variability achieved by the PRM and LSR models respectively with a lower mean achieved by the LSR model. The results achieved so far implies, the ANN models (RBFANN, BPANN and GRNN) predicted heights with greater accuracy and precision than those achieved by the classical models (ARIMA, PRM and LSR).

4 Conclusion

Ellipsoidal height studies have become obligatory in establishing a vertical geodetic reference network for measuring vertical distance. The *h* which has physical meaning is adopted for engineering and mapping purposes. This study applies and assess the performance of soft computing techniques namely, GRNN, BPANN, GRNN to conventional techniques namely, PRM, ARIMA and MLR in estimating local ellipsoidal heights for the GKMA local geodetic reference datum. After comparing the soft computing techniques to the conventional methods based on their statistical analysis and hypothesis testing, it was revealed that the soft computing techniques outperform the conventional methods in estimating a local ellipsoidal height for the area. RBFANN and BPANN compared to GRNN, PRM, ARIMA, and LSR, showed superiority in estimating the heights with much accuracy and precision. We conclude that, utilizing soft computing techniques in estimating local ellipsoidal heights for the study area have proven to be an alternative realistic technique to the conventional techniques. These techniques will help geospatial professionals within the study area catchment and Ghana to know the efficacy of utilizing soft computing techniques in estimating a precise ellipsoidal height for geodetic purposes. However, more work should be done in Ghana utilizing other soft computing techniques which were not considered in this study such as deep learning Convolutional Neural Networks (CNN), Least Squares Support Vector Machines, Extreme Learning Machine to classical improve regression techniques such as Gaussian regression and Kernel Ridge Regression to evaluate its effectiveness for larger engineering projects since the classical techniques of obtaining vertical distances are costly, time consuming and laborious. The propose models could be adopted for estimating heights for topographical mapping to generate Digital Elevation Models (DEM) and also for surface volume computations which requires less accuracy. This study will create the opportunity for geodesist in Ghana to know the efficiency of soft computing techniques in solving some problems related to heights issues in geodesy.

References

Abeho, D.R., Hipkin, R., Tulu, B.B., 2014. Evaluation of EGM08 by means of GPS levelling Uganda. South African Journal of Geomatics 3 (3), 272–284.

Acheamfour, L.B., Tetteh, J., 2014. 2010 Population and Housing Census, District Analytical Report, Kumasi Metropolitan. Ghana Statistical Service.

Ahmadi, M.M.Y.B., Safari, A., Shahbazi, A., Foroughi, I., 2016. On the Comparison of Different Radial Basis Functions in Local Gravity Field Modelling using Levenberg-Marquardt Algorithm. European Geosciences Union General Assembly 2016, Vienna, Austria, 17-22 April 2016, 1–2.

Akcin, H., Celik, C.T., 2013. Performance of Artificial Neural Networks on Kriging Method in Modelling Local Geoid. Boletim de Ciencias Geodesicas 19 (1), 84-97.

Akyilmaz, O., Ozludemir, M.T., Ayan, T., Celik, R.N., 2009. Soft Computing Methods for Geoidal Height Transformation. Earth, Planets and Space 61, 825-833.

Al-Krargy, E.M., Mohamed, H.F., Hosney, M.M., Dawod, G.M., 2017. A High-Precision Geoid for Water Resources Management: A Case Study in Menofia Governorate, Egypt. National Water Research Center (NWRC) Conference on: Research and Technology Development for Sustainable Water Resources Management, Cairo, Egypt, 1-13.

Annan, R.F., Ziggah, Y.Y., Ayer, J., Odutola, C.A., 2016. Accuracy Assessment of heights obtained from Total station and level instrument using Total Least Squares and Ordinary Least Squares Methods. Journal of Geomatics and Planning 3 (2), 87-92.

Arthur, C.K., Temeng, V.A., Ziggah, Y.Y., 2019. Soft Computing – Based Techniques as a Predictive tool to Estimate Blast-Induced Ground Vibration. Journal of Sustainable Mining 18 (4), 287-296.

Atayi, J., Kabo-bah, A. T., & Resources, N., 2018. Assessing the Impacts of Urbinization on the Climate of Kumasi. May 2020. https://doi.org/10.20944/preprints201809.0059.v1

Ayer, J., Agyemang, A.B., Yeboah, F., Osei Jnr, E.M., Abebrese, S., Suleman, I., 2016. A Comparative Analysis of Extracted Heights from Topographic Maps and Measured Reduced Levels in Kumasi, Ghana. South African Journal of Geomatics 5 (3), 313-324.

Bihter, E., 2011. An Automated Height Transformation Using Precise Geoid Models. Scientific Research and Essays 6 (6), 1351-1363.

Box, G.E.P., Jenkins, G.M., 1976. Time Series Analysis: Forecasting and Control. Holden-Day, Boca Raton, Fla, USA.

Cakir, L., Konakoglu, B., 2019. The Impact of Data Normalization on 2D Coordinate Transformation Using GRNN. Geodetski Vestnik 63 (4), 541-553.

Chen, W., Hill, C., 2005. Evaluation Procedure for Coordinate Transformation. Journal of Surveying Engineering 131 (2), 43-49.

Constantin-Octavian, A., 2006. 3D Affine coordinate transformations. Masters of Science Thesis in Geodesy No.3091 TRITA- GIT EX 06-004, School Architecture and the Built Environment,Royal,100 44 Stockholm, Sweden Institute of Technology (KTH), 7.

Dawod, G.M., Al-krargy, E.M., Amer, H.A., 2022. Accuracy Assessment of Horizontal and Vertical Datum Transformations in Small-Areas GNSS Surveys in Egypt. Journal of Research in Environmental and Earth Sciences 8 (1), 19-28.

Dudek, G., 2011. Generalized Regression Neural Network for Forecasting Time Series with Multiple Seasonal Cycles. Springer-Verlag Berlin Heidelberg, 1, 1-8.

El-Rabbany, A., El-diasty, M., Raahemifar, K., 2015. Sequential Tidal Height Prediction Using Artificial Neural Network. October.

Erdogan, S., 2009. A Comparison of Interpolation Methods for Producing Digital Elevation Models at the Field Scale. Earth Surface Processes and Landforms 34, 366-376.

Erol, B., Celik, R.N., 2005. Modelling Local GPS/Levelling Geoid with the Assessment of Inverse Distance Weighting and Geostatistical Kriging Methods. Athens, Greece, 1-5.

Falchi, U., Parente, C., Prezioso, G., 2018. Global Geoid Adjustment on Local Area for GIS Applications Using GNSS Permanent Station Coordinate. Geodesy and Cartography 44 (3), 80-88.

Fu, B., Liu, X., 2014. Application of artificial neural network in GPS height transformation. Applied Mechanics and Materials 501 (504), 2162-2165.

Fusami, A.A., Dodo, J., Ojigi, L., 2021. Modelling Orthometric Height from GPS-Derived Ellipsoidal Height. December 2019.

Gucek, M., Basic, T., 2009. Height Transformation Models from Ellipsoidal into the Normal Orthometric Height System for the Territory of the City of Zagreb. Studia Geophysica et Geodaetica 53, 17-38.

Hannan, S.A., Manza, R.R., Ramteke, R.J., 2010. Generalized Regression Neural Network and Radial Basis Function for Heart Disease Diagnosis. International Journal of Computer Applications 7 (13), 7-13.

Herbert, T., Ono, M.N., 2018. A Gravimetric Approach for the Determination of Orthometric Heights in Akure Environs, Ondo State, Nigeria. Journal of Environment and Earth Sciences 8 (8), 75-80.

Hornik, K., Stinchcombe, M., White, H., 1989. Multilayer feed forward networks are universal approximators. Neural Networks 2 (5), 359-366.

Idri, A., Zakrani, A., Zahi, A., 2010. Design of Radial Basis Function Neural Networks for Software Effort Estimation. International Journal of Computer Science 4 (7), 11-17.

Kaloop, M.R., Rabah, M., Hu, J.W., Zaki, A., 2017. Using Advanced Soft Computing Techniques for Regional Shoreline Geoid Model Estimation and Evaluation. Marine Georesources & Geotechnology 36 (6), 688-697.

Kao, S. P., Ning, F. S., Chen, C. N., & Chen, C. L., 2017. Using Particle Swarm Optimization to Establish a Local Geometric Geoid Model. Boletim de Ciencias Geodesicas 23(2), 327-337.

Kavzoglu, T., Saka, M.H., 2005. Modelling Local GPS/Levelling Geoid Undulations using Artificial Neural Networks. Journal of Geodesy 78 (9), 520-527.

Kim, T.K., 2015. T test as a parametric statistic. Korean Journal of Anesthesiology 68 (6), 541-546.

Konakoglu, B., Cakır, L., Gokalp, E., 2016. 2D Coordinate Transformation Using Artificial Neural Networks 2d Coordinate Transformation Using Artificial Neural Network. The International Archives of the Photogrammetry, Remote Sensing and Spatial Information Sciences, Volume XLII-2/W1, 2016, 3rd International GeoAdvances Workshop, 16-17 October 2016, Istanbul, Turkey. https://doi.org/10.5194/isprs-archives-XLII-2-W1-183-2016.

Konakoglu, B., Cakir, L., 2018. Generalized Regression Neural Network for Coordinate Transformation. International Symposium on Advancements in Information Sciences and Technologies (AIST), Montenegro, 5th 8th September 2018, 66-78.

Kumar Singh, A., 2015. Topic : F-TEST and Analysis of Variance (ANOVA). University of Lucknow, IV, 1-9.

Kumi-Boateng, B., Peprah, M.S., 2020. Modelling Local Geometric Geoid using Soft Computing and Classical Techniques: A Case Study of the University of Mines and Technology (UMaT) Local Geodetic Reference Network. International Journal of Earth Sciences Knowledge and Applications 2, 166-177.

Kumi-Boateng, B., Ziggah, Y.Y., 2017. Horizontal coordinate transformation using artificial neural network technology- A case study of Ghana geodetic reference network. 11(1), 1–11.

Kwak, S.G., Kim, J.H. 2017. Central limit theorem: the cornerstone of modern statistics. Korean Journal of Anesthesiology 70 (2), 144-156.

Lee, J.M., Min, K.S., Min, W.K., Park, H., 2020. A Study on the Actively Capture of Road Construction Information Using Spatial Analysis. Journal of the Korean Society of Cadastre 36 (2), 149-159.

Liu, S., Li, J., Wang, S., 2011. A hybrid GPS height conversion approach considering of neural network and topographic correction. International Conference on Computer Science and Network Technology, China, IEEE. https://doi.org/10.1109/ICCSNT.2011.6182386.

Massey, A., Miller, S.J., 2004. Tests of Hypotheses Using Statistics. Mathematics Department Brown University Providence, RI 02912, 1-32.

Mihalache, R.M., 2012. Coordinate Transformation for Integrating Map Information in the New geocentric European system using Artificial Neural Networks. GeoCAD, 1-9.

Miller, S.J., 2006. Methods of Least Squares, Statistics Theory. Cornell University, USA, 3, 1-2.

Mueller, V.A., Hemond, F.H., 2013. Extended artificial neural networks: in-corporation of a priori chemical knowledge enables use of ion selective electrodes for in-situ measurement of ions at environmental relevant levels. Talenta 117 (15), 112-118.

Oduro, C., Kafui, O., Peprah, C., 2014. Analyzing Growth Patterns of Greater Kumasi Metropolitan Area Using GIS and Multiple Regression Techniques Analyzing Growth Patterns of Greater Kumasi Metropolitan Area Using GIS and Multiple Regression Techniques. Journal of Sustainable Development 7 (5), 13-31. https://doi.org/10.5539/jsd.v7n5p13.

Ophaug, V., Gerlach, C., 2017. On the Equivalence of Spherical Splines with Least-Squares Collocation and Stokes's Formula for Regional Geoid Computation. Journal of Geodesy 91 (6), 1-16. https://doi.org/10.1007/s00190-017-1030-1.

Osei-Nuamah, I., Appiah-Adjei, E.K., 2017. Hydrogeological Evaluation Of Geological Formations In Ashanti Region , Ghana. Journal of Science and Technology 37 (1), 34-50.

Peprah, M.S., Kumi, S.A., 2017. Appraisal of Methods for Estimating Orthometric Heights – A Case Study in a Mine. Journal of Geoscience and Geomatics 5 (3), 96-108.

Peprah, M.S., Mensah, I.O., 2017. Performance Evaluation of the

Ordinary Least Square (OLS) and Total Least Performance Evaluation of the Ordinary Least Square (OLS) and Total Least Square (TLS) in Adjusting Field Data : An Empirical Study on a DGPS Data. South African Journal of Geomatics 6 (1), 73-89.

Pikridas, C., Fotiou, A., Katsougiannopoulos, S., Rossikopoulos, D., 2011. Estimation and evaluation of GPS geoid heights using an artificial neural network model. Applied Geomatics 3, 183-187. https://doi.org/10.1007/s12518-011-0052-2.

Poku-Gyamfi, Y., 2009. Establishment of GPS Reference Network in Ghana. MPhil Dissertation. Universitat Der Bundeswehr Munchen Werner Heisenberg-Weg 39, 85577, Germany, 1-218.

Schaffrin, B., 2006. A note on Constrained Total Least Square estimation. Linear Algebra and Its Application, 417, 245-258.

Specht, D., 1991. A General Regression Neural Network. IEEE Transactions on Neural Networks 6 (2), 568–576.

Srichandan, S., 2012. A New Approach of Software Effort Estimation using Radial Basis Function Neural Networks. International Journal on Advanced Computer Theory and Engineering ISSN (Print) 1 (1), 113-120.

Sureiman, O., Mangera, C.M., 2020. F - Test of Overall Significance in Regression Analysis Simplified. Journal of the Practice of Cardiovascular Sciences 6 (2), 116-122. https://doi.org/10.4103/jpcs.jpcs.

Tusat, E., 2011. A Comparison of Geoid Height Obtained with Adaptive Neural Fuzzy Inference Systems and Polynomial Coefficients Methods. International Journal of the Physical Sciences 6 (4), 789-795.

Ugoni, A., Walker, B.F., 2014. The t TEST An introduction. Comsic Review 4 (2), 37-40.

Veronez, M.R., 2011. Regional Mapping of the Geoid Using GNSS (GPS) Measurements and an Artificial Neural Network. Remote Sensing 668–683. https://doi.org/10.3390/rs3040668.

Veronez, M.R., De Souza, G.C., Matsuoka, T.M., Reinhardt, A., Da Silva, R.M., 2011. Regional Mapping of the Geoid using GNSS (GPS) Measurements and an Artificial Neural Network. Remote Sensing 3 (4), 668-683.

Wu, L., Tang, X., Zhang, S., 2012. The Application of Genetic Neural Network in the GPS Height Transformation. 2012 Fourth International Conference on Computational and Information Science, Beijing, China.

Yakubu, I., Dadzie, I., 2019. Modelling Uncertainties in Differential Global Positioning System Dataset. Journal of Geomatics 13 (1), 16-23.

Yakubu, I., Ziggah, Y.Y., Peprah, M.S., 2018. Adjustment of DGPS Data using artificial intelligence and classical least square techniques. Journal of Geomatics 12 (1), 13-20.

Yilmaz, M., Turgut, B., Gullu, M., Yilmaz, I., 2017. Application of Artificial Neural Networks to Height Transformation. Tehnicki Vjesnik 24 (2), 443-448.

Yonaba, H., Anctil, F., Fortin, V., 2010. Comparing Sigmoid Transfer Functions for Neural Network Multistep Ahead Stream Flow Forecasting. Journal of Hydrologic Engineering 15 (4), 275-283.

Yusof, F., Kane, I.L., Yusof, Z., 2013. Hybrid of ARIMA-GARCH Modelling in Rainfall Time Series. Journal Teknologi 63 (2), 27-34.

Zaletnyik, P., Volgyesi, L., Kirchner, I., Palancz, B., 2007. Combination of GPS/Levelling and the Gravimetric Geoid by using the Thin Plate Spline Interpolation Technique Via Finite Element Method. Journal of Applied Geodesy 1, 223-239.

Ziggah, Y.Y., Youjian, H., Laari, P.B., Hui, Z., 2017. Novel Approach To Improve Geocentric Translation Model Performance Using Artificial Neural Network. Boletim de Ciências Geodésicas 23 (1), 213-233.

Ziggah, Y.Y., Tierra, A., Youjian, H., Konate, A.A., Hui, Z., 2015. Performance Evaluation of Artificial Neural Networks for Planimetric Coordinate Transformation-A Case Study, Ghana. Arabian Journal of Geoscience, 9, 698–714.

Ziggah, Y.Y., Yakubu, I., Kumi-Boateng, B., 2016. Analysis of Methods for Ellipsoidal Height Estimation – The Case of a Local Geodetic Reference Network. Ghana Mining Journal 16 (2), 1-9. https://doi.org/10.4314/gm.v16i2.1.